

MODELING THE EFFECTS OF
HURRICANES ON POWER DISTRIBUTION SYSTEMS

A Thesis

by

SURAJ CHANDA

Submitted to the Office of Graduate Studies of
Texas A&M University
in partial fulfillment of the requirements for the degree of

MASTER OF SCIENCE

August 2011

Major Subject: Electrical Engineering

MODELING THE EFFECTS OF
HURRICANES ON POWER DISTRIBUTION SYSTEMS

A Thesis

by

SURAJ CHANDA

Submitted to the Office of Graduate Studies of
Texas A&M University
in partial fulfillment of the requirements for the degree of
MASTER OF SCIENCE

Approved by:

| | |
|-------------------------|--------------------------------|
| Co-Chairs of Committee, | Alex Sprintson Chanan Singh |
| Committee Members, | Le Xie Emily M.Zechman |
| Head of Department, | Costas N.Georghiades |

August 2011

Major Subject: Electrical Engineering

ABSTRACT

Modeling the Effects of Hurricanes on Power Distribution Systems. (August 2011)

Suraj Chanda, B.E., Osmania University

Co-Chairs of Advisory Committee: Dr. Alex Sprintson
Dr. Chanan Singh

There are many calamitous events such as earthquakes, hurricanes, tsunamis etc. that occur suddenly and cause great loss of life, damage, or hardship. Hurricanes cause significant damage to power distribution systems, resulting in prolonged customer outages and excessive delays in the reconstruction efforts. Accordingly, predicting the effects of power outages on the performance of power distribution systems is of major importance to government agencies, utilities, and customers. Unfortunately, the current tools to predict the performance of power distribution systems during catastrophic events are limited in both the performance measures considered, as well as in their ability to model real systems.

The main goal of this research is to develop a methodology for simulating hurricanes of different intensity on power distribution systems of small and medium size cities. Our study includes a detailed comparison between the engineering-based and connectivity-based models of power distribution systems, as well as the impact of power re-routing algorithms on the system reliability. Our approach is based on fragility curves that capture the ability of the system to withstand a range of wind speeds. In addition, we develop a multiscale approach that facilitates efficient computation of fragility curves for large cities. With this approach, hurricanes are simulated over small zones of a city and fragility curves are obtained. These are used to estimate

the damage for identical zones throughout the city. To validate our techniques, two testbeds, Micropolis and Mesopolis, were used. Micropolis is synthetic model for a small city and Mesopolis for a big city. Obtained results have validated our approach and have shown that they can be used to effectively predict hurricane damage.

To My Loving Family and Friends

ACKNOWLEDGMENTS

I would like to express my sincere gratitude and deepest thanks to my advisors, Alex Sprintson and Chanan Singh. I thank them for their excellent instruction, advice, continuous motivation, encouragement and supervision of my thesis.

I would also like to thank my graduate committee members Le Xie and Emily M. Zechman for their constant monitoring and help they offered at every moment of my thesis work.

Most of all, I would like to thank my family to whom I dedicated this work, especially my parents for their graceful support.

TABLE OF CONTENTS

| CHAPTER | | Page |
|---------|--|------|
| I | INTRODUCTION | 1 |
| | A. Overview | 1 |
| | B. Thesis Outline | 2 |
| II | FRAGILITY CURVES | 4 |
| | A. Regression Analysis vs Fragility Curves | 5 |
| III | LAYOUT OF MICROPOLIS | 7 |
| | A. Layout of the Electrical Infrastructure Components of Micropolis | 8 |
| | B. Layout of the Power Distribution Network of Micropolis . . | 10 |
| IV | ESTIMATING EFFECTS OF HURRICANES | 12 |
| | A. Algorithm | 13 |
| | B. Simulation Inputs and Outputs | 15 |
| | 1. Pole data and line data | 15 |
| | 2. Type of pole material | 15 |
| | 3. Wind speed interval and maximum wind speed | 15 |
| | 4. Confidence interval value | 16 |
| | 5. Outputs | 16 |
| | C. Results | 16 |
| | 1. Effect of hurricanes over single family residenceals . . . | 16 |
| | 2. Effect of hurricanes over multi-family residenceals . . . | 17 |
| | 3. Effect of hurricanes over commercial complexes | 17 |
| | 4. Effect of hurricanes over industries | 18 |
| V | POWER RE-ROUTING | 21 |
| | A. Routing Power Using Normally Open Switches | 21 |
| | 1. Algorithm | 21 |
| | 2. Graphical representation of Micropolis | 23 |
| | 3. Simulation inputs and outputs | 34 |
| | B. Results | 35 |
| | 1. Effect of hurricanes over single family residenceals . . . | 35 |

| CHAPTER | Page |
|--|------|
| 2. Effect of hurricanes over multi-family residentials . . . | 36 |
| 3. Effect of hurricanes over commercial complexes | 39 |
| VI MULTISCALE APPROACH | 44 |
| A. Layout of Mesopolis | 45 |
| 1. Infrastructure components layout | 45 |
| 2. Different layers of Mesopolis | 46 |
| B. Area Considered for Study | 46 |
| 1. Overview of the focused area | 49 |
| 2. Electrical distribution system for focused area | 50 |
| C. Results | 50 |
| 1. Fragility curves showing number of light and medium areas out of power | 50 |
| 2. Comparison of effect of hurricanes over Mesopolis and Micropolis | 52 |
| 3. Estimated fragility curves for light and medium ar- eas throughout Mesopolis | 55 |
| VII DETAILED ENGINEERING MODEL | 59 |
| A. Micropolis Engineering Model | 60 |
| B. Power World and Matlab Interaction | 61 |
| 1. Gauss Seidel method | 62 |
| C. Results | 65 |
| 1. Comparison between engineering model and con- nectivity based model | 65 |
| a. Voltage constraint at a bus is set to 5 percent of nominal voltage | 65 |
| b. Voltage constraint at a bus is set to 10 percent of nominal voltage | 66 |
| VIII CONCLUSION | 70 |
| REFERENCES | 72 |
| APPENDIX A | 74 |
| VITA | 78 |

LIST OF TABLES

| TABLE | | Page |
|-------|---|------|
| I | Voltage profile of customers in Micropolis | 8 |
| II | Load profile of customers in Micropolis | 9 |
| III | Conductor sizing in Micropolis | 24 |
| IV | Sequence impedance and capacitance values for three phase single circuit overhead lines | 28 |
| V | Resistance, inductance and capacitance values for single phase overhead lines | 29 |
| VI | Sequence impedance and capacitance values for three phase dou- ble circuit overhead line | 32 |
| VII | Number of single family residential losing power vs wind speed . . . | 37 |
| VIII | Number of multi-family residential losing power vs wind speed . . . | 39 |
| IX | Number of commercial complexes losing power vs wind speed | 40 |
| X | Assumed average KVA consumption and transformer ratings for different zones | 47 |
| XI | Total light and medium residential in the focused area | 49 |
| XII | Mesopolis light residential normalized calculations | 53 |
| XIII | Mesopolis medium residential normalized calculations | 54 |
| XIV | Micropolis single family residential normalized calculations | 56 |
| XV | When the voltage constraints at a bus are 5% of nominal voltage . . | 67 |
| XVI | When the voltage constraints at a bus are 10% of nominal voltage . . | 69 |

| TABLE | Page |
|--|------|
| XVII Voltage profile of customers in Mesopolis | 77 |
| XVIII Load profile of customers in Mesopolis | 77 |

LIST OF FIGURES

| FIGURE | Page |
|--------|---|
| 1 | Example of a fragility curve 5 |
| 2 | Layout of the Electrical Infrastructure Components 9 |
| 3 | Layout of the Power Distribution Network 10 |
| 4 | Integrated fragility based approach 12 |
| 5 | Fragility curve showing number of single family residential losing power for a given wind speed in the absence of routing 17 |
| 6 | Fragility curve showing number of multi-family residential losing power for a given wind speed in the absence of routing 18 |
| 7 | Fragility curve showing number of commercial complexes losing power for a given wind speed in the absence of routing 19 |
| 8 | Fragility curve showing number of industries losing power for a given wind speed in the absence of routing 20 |
| 9 | Three phase single circuit overhead line conductor configuration . . . 25 |
| 10 | Single phase overhead line conductor configuration 29 |
| 11 | Three phase double circuit overhead line conductor configuration . . 30 |
| 12 | Two phase overhead line conductor configuration 33 |
| 13 | Graphical representation of Micropolis testbed 35 |
| 14 | Fragility curve showing number of single family residential losing power for a range of wind speeds in the presence of routing 36 |
| 15 | Bar graph representing the number of single family residential losing power 38 |

| FIGURE | Page |
|--------|---|
| 16 | Fragility curve showing number of multi-family residentials losing power for a range of wind speeds in the presence of routing 38 |
| 17 | Bar graph representing number of multi-family residentials losing power for a range of wind speeds 41 |
| 18 | Fragility curve showing number of commercial complexes losing power for a range of wind speeds in the presence of routing 42 |
| 19 | Bar graph representing number of commercial complexes losing power for a range of wind speeds 43 |
| 20 | Mesopolis overview 46 |
| 21 | Mesopolis infrastructure layout 47 |
| 22 | Mesopolis roads and freeways layout 48 |
| 23 | Mesopolis pressure zones 48 |
| 24 | Focused area of Mesopolis 49 |
| 25 | Electrical distribution system for considered area of Mesopolis 50 |
| 26 | Fragility curves showing number of light areas out of power for a given wind speed 51 |
| 27 | Fragility Curves showing number of medium areas out of power for a given wind speed 51 |
| 28 | Comparison of effect of hurricanes over Mesopolis and Micropolis 52 |
| 29 | Varying hurricane wind speeds for different areas of the city 55 |
| 30 | Fragility curve showing percentage of medium residentials losing power for a given wind speed 57 |
| 31 | Fragility curve showing percentage of light residentials losing power for a given wind speed 57 |
| 32 | Micropolis power world model 61 |

| FIGURE | | Page |
|--------|--|------|
| 33 | Example of a typical bus in a power system | 63 |
| 34 | Comparison of results from matlab and power world when voltage change allowed is 5% of nominal | 66 |
| 35 | Comparison of results from matlab and power world when voltage change allowed is 10% of nominal | 68 |
| 36 | Paper layouts showing building of Mesopolis | 75 |
| 37 | University, residential areas and port in Mesopolis | 75 |
| 38 | Overview of Mesopolis | 76 |

CHAPTER I

INTRODUCTION

A. Overview

There are many calamitous events such as earthquakes, hurricanes, tsunamis etc. that occur suddenly and cause great loss of life, damage, or hardship. Hurricanes are one of the deadliest disasters. They are also known as cyclones in the northern Indian Ocean and typhoons in the western Pacific Ocean. Some of the dangerous hurricanes in the past are Bhola Cyclone - Bangladesh (1970), Andhra Pradesh Cyclone - India (1977), Cindy - United States (2005), Katrina - United States (2005) etc [1,2]. These disasters have severely affected the power distribution systems of many cities causing power outages and incurring huge capital losses. A hurricane is difficult to predict and analyze as it affects a large area and its speed varies from time to time. A pre-storm analysis would help in estimating of the amount of damage (e.g., broken poles) to power distribution systems during hurricanes.

Accurate and reliable customer outage predictions will suggest the utility company, the course of actions that are necessary to fight the storm conditions. The research work conducted as a part of this thesis proposes a methodology to study and quantify the damage caused by hurricanes to the electrical distribution network of a city.

By introducing efficient simulation algorithms, this thesis proposes a methodology to study the damage caused by hurricanes to the electrical infrastructure. The extent of damage caused to the electrical network by hurricanes of different intensity are quantified by means of fragility curves.

The journal model is *IEEE Transactions on Automatic Control*.

This study has been carried out on two testbeds comprising of all infrastructural components which were laid out using a Geographic Information System (GIS) based software package by researchers at the Department of Civil Engineering and the Department of Electrical and Computer Engineering at Texas A&M University [3,4].

B. Thesis Outline

The main emphasis of the research is to develop effective algorithms that simulate hurricanes of different wind speeds and analyze the resulting fragility curves generated. This information is used to estimate the intensity of a hurricane of particular wind speed and its effects over the power distribution system of a city. The rest of this thesis is organized as follows:

Chapter II describes the concept of fragility curves and their applications in estimating the resilience of a real system. The advantages of Monte Carlo method over the Latin hypercube method is presented. It also gives a basic comparison between regression analysis and the fragility curves.

Chapter III introduces the layout of the first testbed under consideration, Micropolis. The parameters like ratings, voltage levels, type of conductors used for overhead lines etc., are discussed. The layout of the electrical infrastructure components and the layout of the power distribution network of Micropolis are presented.

Chapter IV introduces the algorithms used in simulating the effect of hurricanes on the testbed. This chapter deals with the settings where there is no routing involved.

Chapter V introduces a power re-routing algorithm which estimates the effect of hurricanes in the presence of routing. The graph model is presented and the method of routing implemented is discussed.

Chapter VI introduces a multiscale approach in simulating hurricanes over small zones of a city and using the generated fragility curves to estimate the damage for similar zones throughout the city. For this purpose a large testbed, Mesopolis is considered. The parameters like ratings, voltage levels, type of conductors used for overhead lines etc., are discussed. The layout of the electrical infrastructure components and the layout of the power distribution network of Mesopolis are presented.

Chapter VII compares between engineering and connectivity models. It introduces the detailed engineering model built using Power World Simulator [5]. It presents the important parameters, constraints and conditions considered for building this model. The comparison of the results from connectivity-based and engineering models are analyzed.

Chapter VIII presents conclusions, and highlights possible future research in this field.

CHAPTER II

FRAGILITY CURVES

The fragility of a structure is mathematically defined as the probability of failure of the structure conditional on a specific parameter. We focus on fragility curves of poles, which are one of the major components of power distribution systems. Fragility curves for poles describe the likelihood of damage of poles made of a particular material at different wind speeds.

The main objective of this chapter is to demonstrate a methodology for generating fragility curves for a small city using the Monte Carlo method. The methodology is based on several simplifying assumptions. Most important assumption made is that all the faults occurring in the system are considered as short circuit faults. This implies that for a fault on a pole, all the lines associated with the pole are said to be down and all the customers feeded by that line are out of power. In summary, for analytical fragility curves, there are two ways of computing probabilities of damage. The most direct and accurate means uses Monte Carlo technique to simulate a large number of random samples and calculate probability by counting the actual outcomes. This is a brute-force method that provides accurate values of probability of damage, but it is very computational expensive. Another means uses a sampling technique such as a Latin hypercube to simplify the random simulation process. It significantly reduces the number of samples to a manageable level and approximates the probability values by curve-fitting a small number of responses to an assumed probability distribution. However, in this research Monte Carlo method is followed due to the requirement of highly accurate results.

Example of fragility curve is shown in Fig. 1 [3]. This curve indicates the probability of failure ($p(f)$) for a range of wind speeds for power system poles.

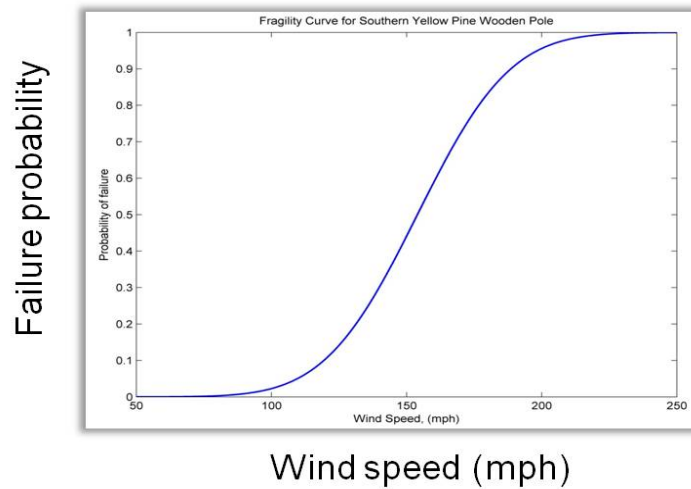


Fig. 1. Example of a fragility curve

A. Regression Analysis vs Fragility Curves

Main features of Regression Analysis are as follows:

1. Models event as function of many different influences like wind load, soil moisture, land use, etc.
2. Captures broad range of influences [6].
3. Based primarily on observed performance data.
4. Focuses on end point of interest like outage, customer meter out, pole damage.
5. Its a top to bottom approach.

In contrast to the above, important features of fragility curves are:

1. Model event as function of a single demand parameter (such as wind speed) and captures only one influence on failure.
2. Generally assume conditional independence of events given single-value loading.

3. Focus on physical damage couple with topology to estimate end point of interest.
4. It is a bottom to top approach.

CHAPTER III

LAYOUT OF MICROPOLIS

To validate our techniques, two testbeds Micropolis and Mesopolis were developed using GIS (ArcMap) and hydraulic modeling (EPANet) based software [4]. Developing a complete testbed with all the important infrastructural components embedded is one of the important aspects of this research. The virtual city of Micropolis, as represented by the layout of Fig. 2 was designed to serve as a testbed for carrying out studies on the effects of disasters on the interdependent infrastructure components of a city. The electrical distribution network of the city was then modeled and its corresponding components added to the GIS layout. The features of Micropolis testbed are as follows:

1. A city of around 5000 residents.
2. It covers an area of approximately 2 square miles.
3. Micropolis does not have its own power generation facility. So a sub-transmission line (138 KV rating) running through the city provides power to the entire city.
4. City has one substation where the voltage is stepped down to 13.8 kV.
5. Two three phase feeders go from substation into the city. Later each one is divided into small branches which feed the end customers. Each of them is of 13.8 kV rating.
6. Left part of the city has underground cables and in this case pad mounted transformers (100kVA and above rating) are used. These cables are represented with dotted lines.

Table I. Voltage profile of customers in Micropolis

Voltage Profiles

| Customer Type | Voltage Ratings |
|--------------------------------------|---------------------------------------|
| Residential (Feeders 1 & 2) | 120V, 1 – ϕ |
| City Churches and Schools | 208V, 3 – ϕ |
| Industrial (Feeder 1) | 208V, 3 – ϕ or 3.3KV, 3 – ϕ |
| Central Business District (Feeder 2) | 208V, 3 – ϕ |

7. Right part of the city has overhead lines supported by wooden poles. These are represented by solid lines and the poles are represented with yellow dots.
8. City is designed down to individual household level, based on 130 year development history. But this time line wont impact the electrical model as the electrical components are upgraded or replaced every 40 to 50 years.

Table I shows the voltage profiles of customers in Micropolis. Table II shows the load profiles of customers in Micropolis.

A. Layout of the Electrical Infrastructure Components of Micropolis

Due to its small size, Micropolis does not have its own power generation facility. So a sub-transmission line running through the city provides power to the entire city. City has one substation with two feeders going from substation into the city. Left part of the city has underground cables which are represented with dotted lines. Right part of the city has overhead lines supported by wooden poles which are represented by

Table II. Load profile of customers in Micropolis

Load Profiles

| Customer Type | Load Consumed |
|--------------------------------------|-------------------|
| Residential (Feeder 1) | 5 KVA |
| Residential (Feeder 2) | 7 KVA |
| City Churches | 250 KVA |
| City Schools | 300 KVA |
| Industrial (Feeder 1) | 30/75/150/22 KVA |
| Central Business District (Feeder 2) | 30/45/150/250 KVA |

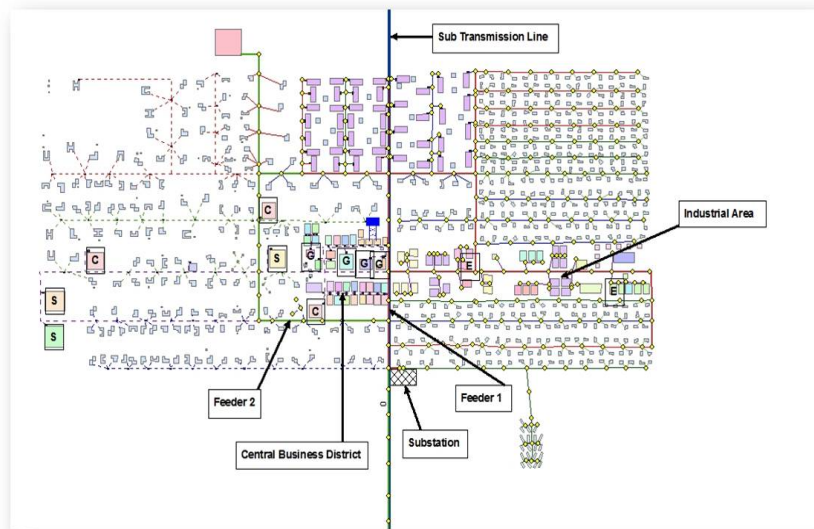


Fig. 2. Layout of the Electrical Infrastructure Components

solid lines and the poles with yellow dots.

B. Layout of the Power Distribution Network of Micropolis

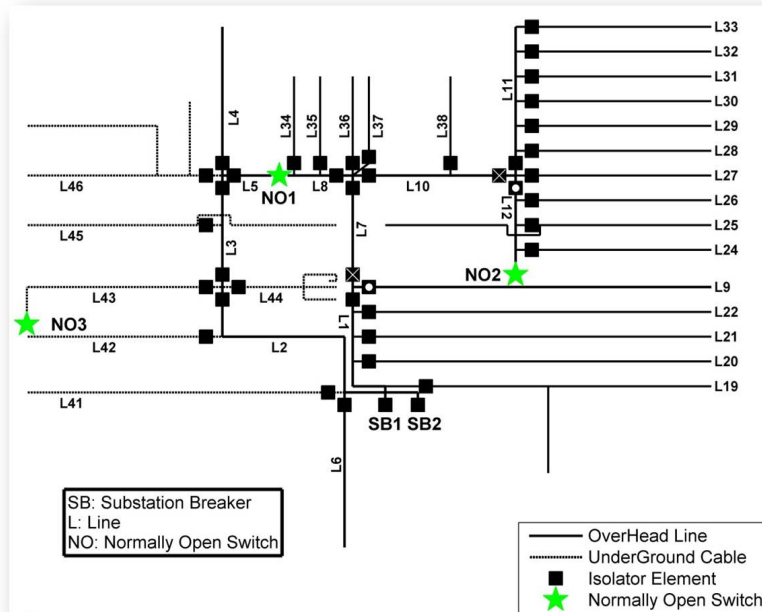


Fig. 3. Layout of the Power Distribution Network

The layout of the electrical distribution network of Micropolis is as shown in Fig. 3. A line can be defined as a switchable section of the network with one or more isolating elements at its ends [7]. These isolators are assumed to be manually operated and ensure safe tripping of a faulted line. The utility engineers depend on personal calls in order to locate a particular fault, before isolating it physically and carry out repair and restoration services. The substation breakers of the distribution network, however, are assumed to be operated through over-current relays. In the event that a short circuit fault occurs at some point in the distribution system, the relay trips the breaker open. After a sufficient delay during which the maintenance

personnel are assumed to have located and isolated the concerned fault, the breaker is closed in order to restore service to the remaining parts of the network. Various users across Micropolis have been categorized into different profiles (e.g. residential, commercial, industrial etc.) [3], and it is assumed that the customers belonging to each such profile have a fixed load demand (KVA) all through the year. The different load profiles are as shown in Table II. It is further assumed that the local electric utility maintains a constant power factor of 0.95 for all load points across the city. Thus, all buildings connected to a given distribution transformer are modeled in the testbed as a single load point with a fixed KW and KVAR demand associated with it [5].

CHAPTER IV

ESTIMATING EFFECTS OF HURRICANES

As seen in the Fig. 4 an Integrated Fragility-based Approach is followed to estimate the customer outages by type and location. In the Micropolis testbed there are four

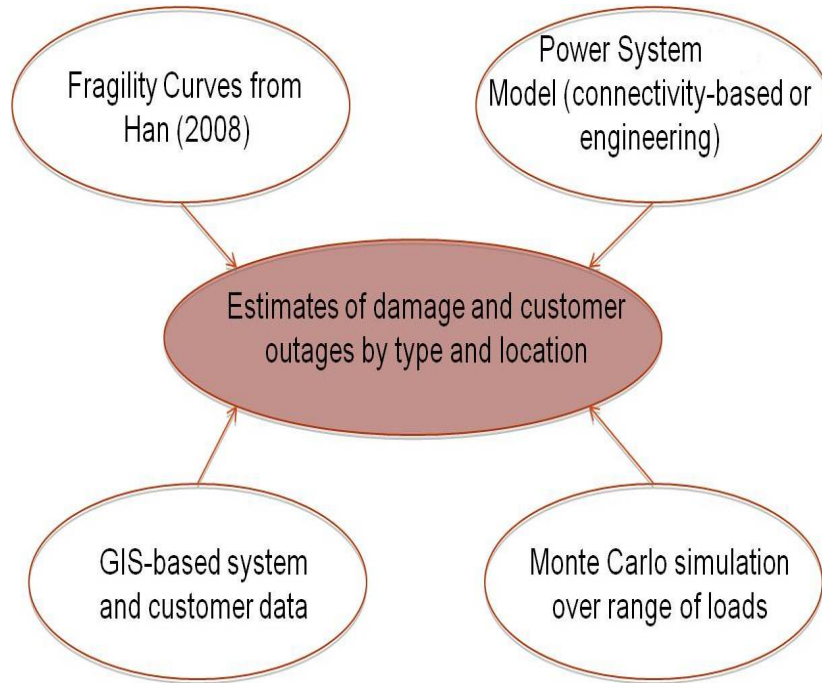


Fig. 4. Integrated fragility based approach

types of customers. They are single family residential (represented by a variable ‘sfr’), multi family residential (represented by a variable ‘mfr’), commercial complexes (represented by a variable ‘comm’) and industries (represented by a variable ‘in’). All the poles in the Micropolis are assumed to be made of Southern Pine wood. So the mean and standard deviation are fixed as all the poles are of same material. Hence the probability of failure can be easily found out by finding the cumulative distribution function with wind speed, mean and standard deviation as parameters. Then using Monte Carlo method, several simulations are run and finally the fragility

curves are plotted to study the effect of hurricanes on the testbed.

The distribution systems usually have a radial topology. In this scenario, though there are three normally open switches located across the electrical distribution network of Micropolis (as shown in Fig. 3), they are assumed to be non-functional for the time being. The Micropolis electrical distribution system is assumed to be connected to an infinite bus, so that events like a sudden loss of system load does not cause any system stability issues. Since there is no re-routing considered in this case, the damage is severe and once a line is out of power, customers fed by that line are out of power permanently. This is a more general case where no complexities are involved as the normally open switches are considered as open all the time.

A. Algorithm

Electrical simulation algorithm is developed such that it accommodates all the assumptions considered. It is as follows:

1. Read the mean and standard deviation for a given type of material used for making poles.
2. Determine which all poles are down for a particular wind speed depending on the probability of failure of wood made of a particular material.
3. Determine all lines that are affected by the faulted poles.
4. Scan all Line numbers as found in step (3) to determine which of those are downstream with respect to the others. Eliminate all such downstream Line numbers from the list of (3) as they will anyways be getting isolated by the isolation of their concerned upstream components.

5. Isolate each of the upstream Lines as identified in step (4). For each such isolated upstream component, scan all Lines which are located downstream to it. In this process all the down stream lines of a faulted line are automatically isolated.
6. For each isolated Line calculate the total number of customers losing power. As there are four types of customers, individually calculate total number of customers losing power for each type (sfr, mfr, comm and in).
7. Are all upstream Lines as found in step (4) isolated? If yes, go to (8). If not, go to (5).
8. Store all the types of customers out of power in four different variables.
9. Run the algorithm for wind speed in the range of 50mph to 200mph with specified intervals.
10. The number of Monte Carlo simulations to be run depends on the required accuracy.

The above mentioned algorithm is then used to implement the methodology proposed in this chapter for studying and quantifying the damage caused by hurricanes to the electrical network. The following chapter discusses all relevant results obtained from running numerous simulations on the Micropolis electrical distribution system, corresponding to different hurricane wind speeds.

B. Simulation Inputs and Outputs

1. Pole data and line data

Most important input to the algorithm is the pole and line information. This is fed to the algorithm in the form of matrices. The pole info matrix contains the following data:

1. Pole number and the lines on which the pole is located.
2. Transformer rating if there is any transformer connected to the pole.
3. Corresponding ID for the pole used for representation in GIS Arcmap.

The Line info matrix contains the following data:

1. Line number and the numbers of downstream lines to it.
2. Number of single family residences, multi family residences, commercial complexes and industries fed by a line.
3. Corresponding ID for the Line used for representation in GIS Arcmap.

2. Type of pole material

In this case the material used to make a pole is southern pine wood. So the mean and standard deviation are given as inputs to calculate Normal Distribution function to estimate the probability of failure used later in the algorithm.

3. Wind speed interval and maximum wind speed

As discussed in the algorithm, a range of wind speed is required as input. Speed of 50mph is considered as the minimum wind speed of hurricanes in this case. So

wind speed interval and maximum wind speed must be given as inputs to drive the simulation.

4. Confidence interval value

Confidence interval (CI) is a particular kind of interval estimate of a population parameter and is used to indicate the reliability of an estimate. It is an observed interval (i.e., it is calculated from the observations), in principle different from sample to sample, that frequently includes the parameter of interest, if the experiment is repeated. In this case confidence interval value of 95 percent is used.

5. Outputs

After the algorithm is run for a set of Monte Carlo simulations over a range of wind speeds, the outputs are four matrices of single family residential (sfr), multi-family residential (mfr), commercial complexes (comm) and industries(in) that have the information regarding the number of entities of a particular type losing power for all the wind speeds. This information is used to develop fragility curves.

C. Results

1. Effect of hurricanes over single family residential

The Fig. 5 shows the fragility curve plotted for the case where routing is absent. On observation, the number of houses losing power increases along with the wind speed. Around a high wind speed of 150 mph, the curve saturates. At this speed, all the single family residential in the city are out of power. Confidence interval of 95% is plotted for the fragility curves. This shows that for wind speeds of 150 mph and above all single family residential will be out of power.

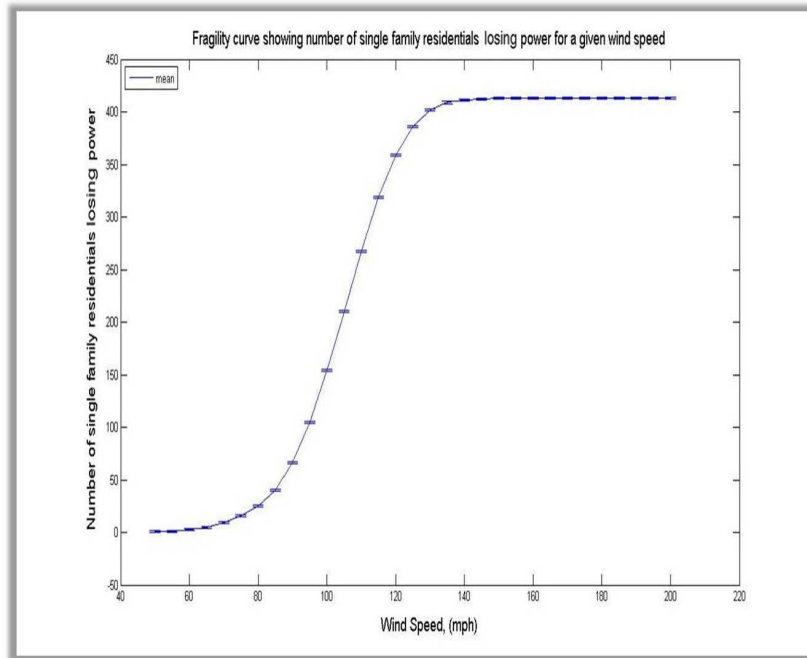


Fig. 5. Fragility curve showing number of single family residential losing power for a given wind speed in the absence of routing

2. Effect of hurricanes over multi-family residentials

The Fig. 6 shows the fragility curve plotted for the case where routing is absent. On observation, the number of houses losing power increases along with the wind speed. Around a high wind speed of 130 mph, the curve saturates. At this speed, all the multi-family residentials in the city are out of power. Confidence interval of 95% is plotted for the fragility curves. This shows that for wind speeds of 130 mph and above all multi-family residentials will be out of power.

3. Effect of hurricanes over commercial complexes

The Fig. 7 shows the fragility curve plotted for the case where routing is absent. On observation, the number of commercial complexes losing power increases along with the wind speed. Around a high wind speed of 135 mph, the curve saturates. At this

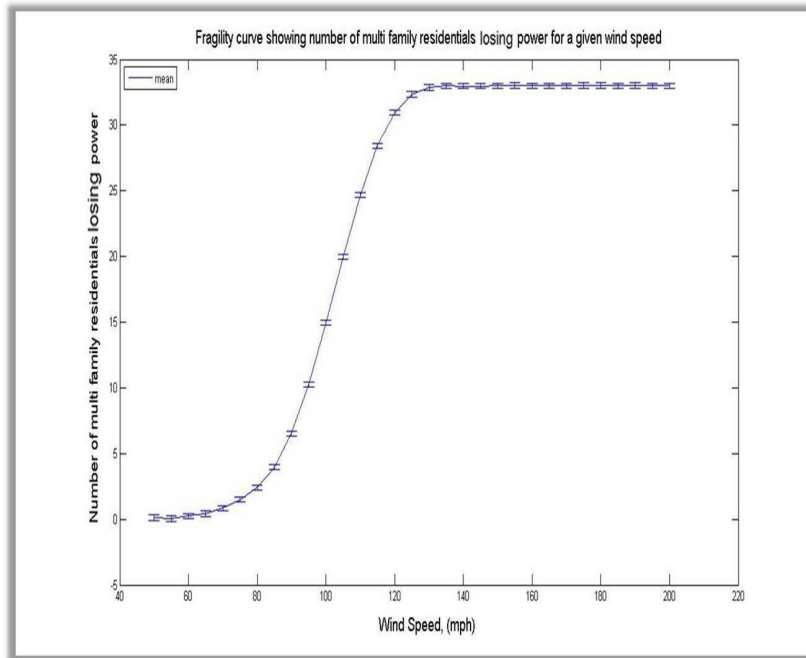


Fig. 6. Fragility curve showing number of multi-family residential losing power for a given wind speed in the absence of routing

speed, all the commercial complexes in the city are out of power. Confidence interval of 95% is plotted for the fragility curves. This shows that for wind speeds of 140 mph and above all commercial complexes will be out of power.

4. Effect of hurricanes over industries

The Fig. 8, shows the fragility curve plotted for the case where routing is absent. On observation, the number of industries losing power increases along with the wind speed. Around a wind speed of 120 mph, the curve saturates. At this speed, all the industries in the city are out of power. Confidence interval of 95% is plotted for the fragility curves. This shows that for wind speeds of 150 mph and above all industries will be out of power.

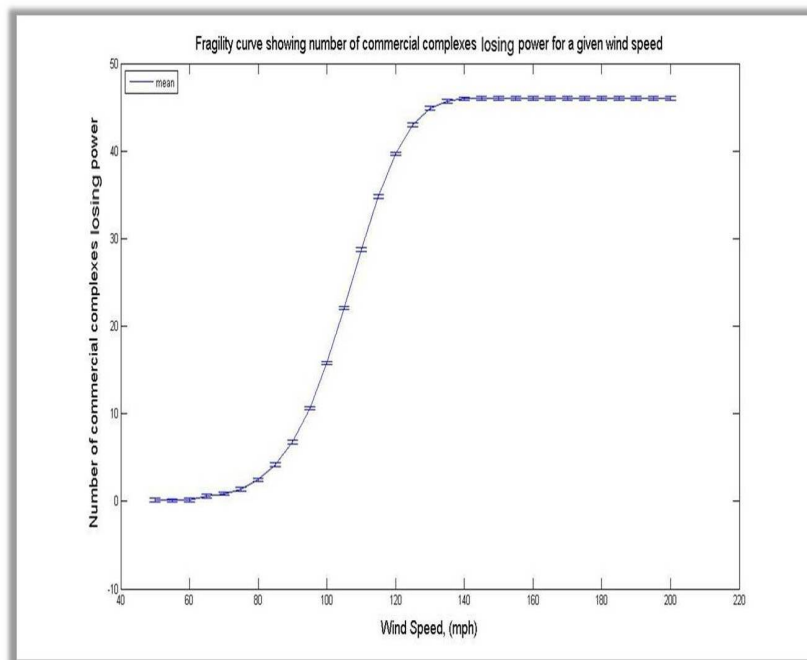


Fig. 7. Fragility curve showing number of commercial complexes losing power for a given wind speed in the absence of routing

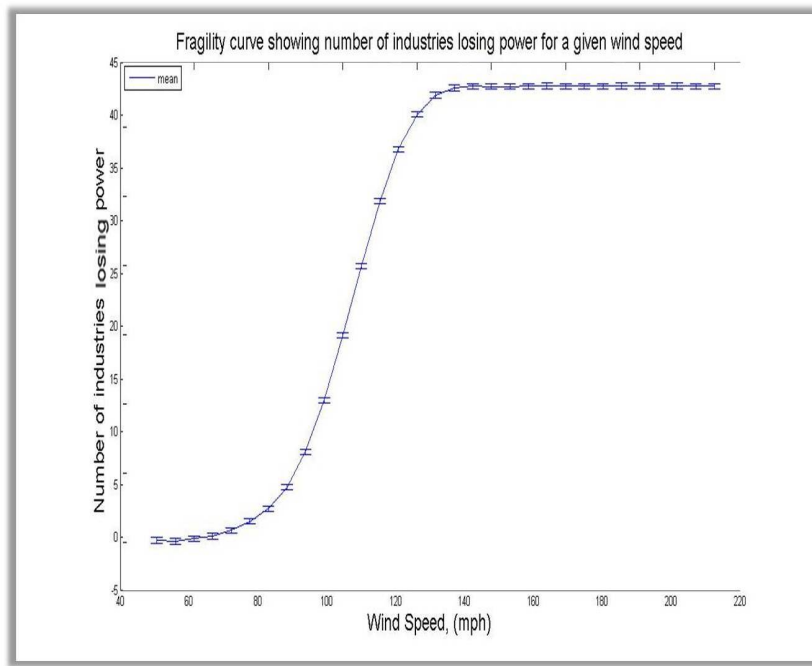


Fig. 8. Fragility curve showing number of industries losing power for a given wind speed in the absence of routing

CHAPTER V

POWER RE-ROUTING

In this scenario, the three normally open switches located across the electrical distribution network of Micropolis (as shown in Fig. 3) are functional. The Micropolis electrical distribution system is assumed to be connected to an infinite bus, so that events like a sudden loss of system load do not cause any system stability issues. This is a more complex scenario compared to previous one as one has to decide a method of using the normally open switches effectively so that at a particular time routing of power should be done to all the possible parts of the city. For this problem, graph solution is applied and discussed in this chapter.

A. Routing Power Using Normally Open Switches

An algorithm is developed which enables routing in a hurricane hit scenario by using all the available normally open switches in the city.

1. Algorithm

This section presents a power routing algorithm by including the normally open switches available in the city. This algorithm is an extension of the one discussed in previous section. It considers the impedance values of the lines as weights and uses a matlab command to build a biograph model of the system. Then shortest path is found using the information of normally open switches present in the city. Initially all the normally open switches are assigned a high value. The sequence of steps are as follows:

1. Read the mean and standard deviation for a given type of material used for

making poles.

2. Determine which all poles are down for a particular wind speed depending on the probability of failure of wood made of a particular material.
3. Determine all lines that are affected by the faulted poles.
4. Determine the faulted nodes from the faulted line numbers obtained from (3).
5. For each wind speed, form an array that stores all the faulted nodes.
6. Using these faulted nodes from (5) determine the number of normally open switches to be closed for maximum power routing.
7. Develop a graph for the system under consideration and find the shortest path for routing. In this case all the weights of closed normally open switches are replaced with zeros.
8. Store the line numbers which are routed and subtract them from lines obtained from (3).
9. Scan all line numbers as found in step (3) to determine which of those are downstream with respect to the others. Eliminate all such downstream line numbers from the list of (3) as they will be getting isolated by the isolation of their concerned upstream components.
10. Isolate each of the upstream lines as identified in step (9). For each such isolated upstream component, scan all Lines which are located downstream to it. In this process all the down stream lines of a faulted line are automatically isolated.

11. For each isolated Line calculate the total number of customers losing power. As there are four types of customers, individually calculate total number of customers losing power for each type (sfr, mfr, comm and in).
12. Are all upstream Lines as found in step (9) isolated? If yes, go to (8). If not, go to (13).
13. Store all the types of customers out of power in four different variables.
14. Run the algorithm for wind speed range 50mph to 200mph with specified intervals.
15. The number of Monte Carlo simulations to be run depends on the required accuracy.

2. Graphical representation of Micropolis

A graph model is analyzed for Micropolis testbed. This section presents the parameters used for building the graph model and their derivation. Later this graph model is used to find the shortest path and route power to faulted sections of the city using the three normally open switches present in the city. Assigning weights is the most crucial part of a graph. These weights are assigned depending on the impedance values of the lines in the system. Table III shows the ampacity for different sizes of conductors considered. These values are used to calculate the impedances. The following cases show the calculation of impedance for different types of overhead lines in Micropolis.

1. Three phase single circuit overhead lines: In the electrical distribution network of Micropolis, it is assumed that all three phase single circuit overhead lines present have the same conductor configuration as shown in the below figure and the primitive impedance matrix ' Z_{prim} ' for this configuration is calculated

Table III. Conductor sizing in Micropolis

Overhead Lines

| Conductor Size | Ampacity (Amps) |
|--------------------------|-----------------|
| 6AWG ^b | 110 A |
| 2 AWG | 195 A |
| 3/0 AWG | 350 A |
| 4/0 AWG | 410 A |
| 266.8 kcmil ^c | 475 A |
| 397.5 kcmil | 615 A |

as below:

$$Z_{prim} = \begin{bmatrix} z_{aa} & z_{ab} & z_{ac} & z_{an} \\ z_{ba} & z_{bb} & z_{bc} & z_{bn} \\ z_{ca} & z_{cb} & z_{cc} & z_{cn} \\ z_{na} & z_{nb} & z_{nc} & z_{nn} \end{bmatrix} \quad (5.1)$$

$$z_{ii} = r_i + 0.0953 + j * 0.12134 * \log_e((1/GMR_i) + 7.934) \Omega/\text{mi} \quad (5.2)$$

$$z_{ij} = 0.0953 + j * 0.12134 * \log_e((1/GMD) + 7.934) \Omega/\text{mi} \quad (5.3)$$

Equation 5.2 is used to compute the diagonal elements of matrix Z_{prim} , whereas Equation 5.3 is used to calculate the off diagonal elements. In equation 5.2, ' r_i ' is the conductor resistance in ohms/mile and ' GMR_i ' is the conductor geometric mean radius in feet. If we assume all the conductors are ideally transposed, the GMD (Geometric Mean Distance) in Equation 5.3 for all off-diagonal terms of

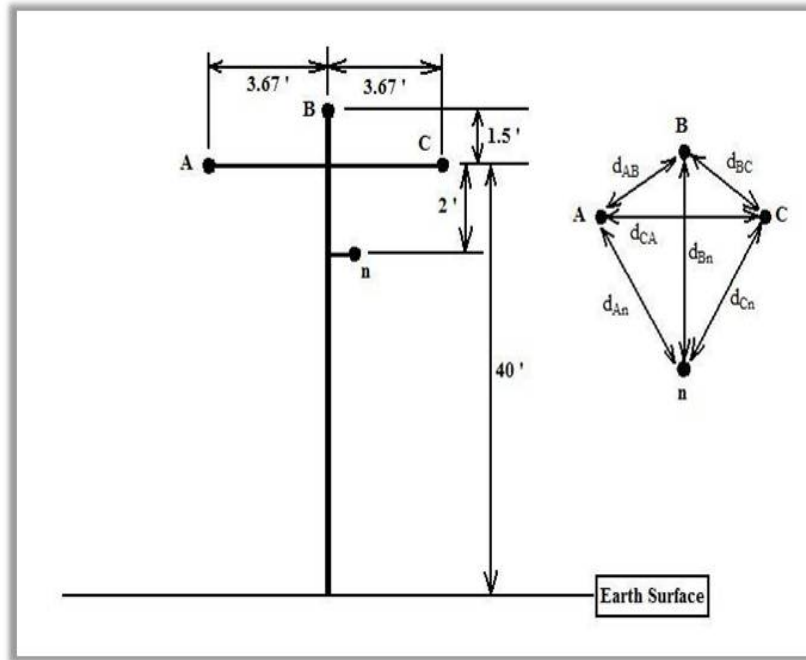


Fig. 9. Three phase single circuit overhead line conductor configuration

matrix Z_{prim} involving any two phase conductors is equal to $\sqrt[3]{d_{AB} * d_{BC} * d_{CA}}$. GMD for all off-diagonal terms involving a phase conductor and the neutral is equal to $\sqrt[3]{d_{An} * d_{Bn} * d_{Cn}}$ (Refer Fig. 9). Using Kron reduction, the [4X4] primitive impedance matrix is then reduced to a [3X3] phase impedance matrix ' Z_{abc} ' as shown below:

$$Z_{abc} = \begin{bmatrix} Z_{aa} & Z_{ab} & Z_{ac} \\ Z_{ba} & Z_{bb} & Z_{bc} \\ Z_{ca} & Z_{cb} & Z_{cc} \end{bmatrix} \quad (5.4)$$

$$Z_{ij} = z_{ij} - (z_{in} * z_{nj}) / z_{nn} \quad (5.5)$$

The elements of matrix Z_{abc} can be calculated by using Equation 5.5, where the terms to the right hand side of the equation refer to those of the matrix

Z_{prim} . A sequence impedance transformation is then performed once Z_{abc} has been calculated in order to obtain the [3X3] sequence impedance matrix ' Z_{012} ' as shown below:

$$Z_{012} = [A^{-1}] * Z_{\text{abc}} * A \quad (5.6)$$

$$A = \begin{bmatrix} 1 & 1 & 1 \\ 1 & a^2 & a \\ 1 & a & a^2 \end{bmatrix} \quad (5.7)$$

In Equation 5.7, the operator 'a' represents the complex quantity $e^{j*(2*\pi/3)}$. The calculated sequence impedance matrix has the following diagonal structure, where ' Z_0 ' represents the zero sequence impedance of the concerned overhead line and ' Z_1 ' the positive sequence impedance.

$$Z_{012} = \begin{bmatrix} Z_0 & 0 & 0 \\ 0 & Z_1 & 0 \\ 0 & 0 & Z_2 \end{bmatrix} \quad (5.8)$$

To calculate the sequence capacitance values for three phase overhead lines, the first step is to form the [4X4] potential coefficient matrix ' P_{pot} ' as shown below:

$$P_{\text{pot}} = \begin{bmatrix} p_{aa} & p_{ab} & p_{ac} & p_{an} \\ p_{ba} & p_{bb} & p_{bc} & p_{bn} \\ p_{ca} & p_{cb} & p_{cc} & p_{cn} \\ p_{na} & p_{nb} & p_{nc} & p_{nn} \end{bmatrix} \quad (5.9)$$

$$p_{ii} = (1/(2 * \pi * \epsilon_o)) * \log_e(2 * h_i/r_i) \text{ km/nF} \quad (5.10)$$

$$p_{ij} = (1/(2 * \pi * \epsilon_o)) * \log_e(D_{ij}/d_{ij}) \text{ km/nF} \quad (5.11)$$

The Equation 5.10 is used to compute the diagonal elements of matrix P_{pot} , while the Equation 5.11 is used to calculate the off-diagonal elements. In Equation 5.10, ' h_i ' represents the average height above ground (feet) of conductor 'i' (see Fig. 9); where as ' r_i ' is the conductor radius in feet. In Equation 5.11, ' D_{ij} ' is the distance between the conductor 'i' and the image below earth surface of the conductor 'j' in feet, and ' d_{ij} ' is the distance in feet between the conductors 'i' and 'j' (see Fig. 9). ' ϵ_o ' is the permittivity of free space and is equal to 8.854 nF/km. Using the Kron reduction formula in Equation 5.5, the [4X4] potential coefficient matrix is then reduced to a [3X3] matrix ' P_{red} '. By inverting matrix P_{red} we obtain the capacitance matrix ' C_{red} '. Thus, $C_{\text{red}} = [P_{\text{red}}]^{-1}$ nF/km. The sequence capacitance values are calculated by performing a sequence admittance transformation on the matrix C_{red} , using the same procedure as was outlined through equations Eq 5.6 , Eq 5.7. Thus,

$$C_{012} = [A^{-1}] * C_{\text{red}} * A \quad (5.12)$$

Table IV shows the calculated values of sequence impedance and capacitance values associated with the different three phase overhead lines present in the electrical distribution network of Micropolis.

2. Single phase overhead lines: All single phase overhead lines of Micropolis are assumed to have the same conductor configuration as shown in the below Fig. 10. The value of the conductor resistance (Ω/km) is obtained from standard tables. The inductance per conductor and the capacitance across the conductors

Table IV. Sequence impedance and capacitance values for three phase single circuit overhead lines

| Conductor Size | $Z_1(\Omega/\text{km})$ | $Z_0(\Omega/\text{Km})$ | $C_1(\text{nF}/\text{Km})$ | $C_0(\text{nF}/\text{Km})$ |
|----------------|-------------------------|-------------------------|----------------------------|----------------------------|
| 6 AWG | $2.64 + j * 0.51$ | $3.0341 + j * 1.8$ | 8.66 | 4.64 |
| 2 AWG | $1.04 + j * 0.47$ | $1.5173 + j * 1.49$ | 9.33 | 4.90 |
| 3/0 AWG | $0.41 + j * 0.44$ | $0.7597 + j * 1.17$ | 10.1 | 5.19 |
| 4/0 AWG | $0.32 + j * 0.43$ | $0.6285 + j * 1.12$ | 10.35 | 5.27 |
| 4266.8 kcmil | $0.26 + j * 42$ | $0.5171 + j * 1.08$ | 10.58 | 5.35 |
| 397.5 kcmil | $0.17 + j * 0.40$ | $0.3702 + j * 1.02$ | 11.03 | 5.51 |

of Fig. 10 are calculated as

$$L_\phi = 0.2 * \log_e(GMD/GMR) \text{ mH/km}$$

$$C_{\phi-n} = 1/(36 * \log_e(D/r)) \mu\text{F/km} \quad (5.13)$$

In Equation 5.13, ‘GMR’ is the conductor’s geometric mean radius expressed in feet, ‘r’ is the physical radius of the conductor expressed in feet and ‘D’ is the distance of separation between the conductors in feet [8]. By assuming that both the phase and the neutral conductors have the same cross-section area and number of strands, the term ‘GMD’ in Equation 5.13 is approximately equal to the distance of separation between the two conductors [9]. Table V shows the calculated resistance, inductance and capacitance values associated with the different single phase overhead lines present in the electrical distribution network of Micropolis.

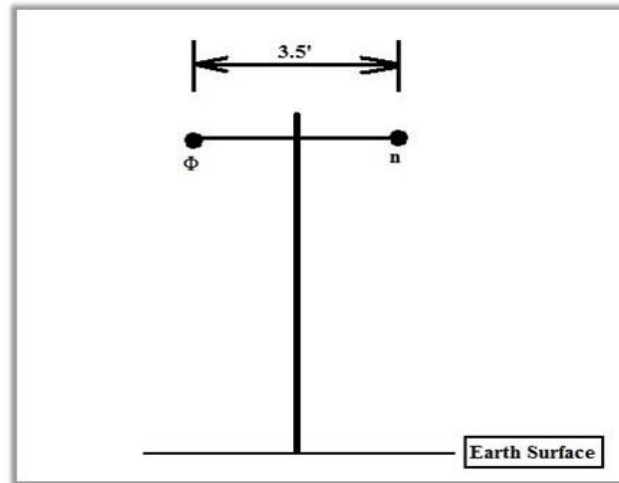


Fig. 10. Single phase overhead line conductor configuration

Table V. Resistance, inductance and capacitance values for single phase overhead lines

| Conductor Size | $R(\Omega/\text{km})$ | $L(\text{mH}/\text{Km})$ | $C(\text{nF}/\text{Km})$ |
|----------------|-----------------------|--------------------------|--------------------------|
| 6 AWG | 2.6411 | 1.2876 | 4.5362 |
| 2 AWG | 1.0433 | 1.1972 | 4.9062 |

3. Three phase double circuit overhead line: In a double circuit configuration, the distribution feeders of Micropolis run for some distance from the substation, before going into their respective service areas. The concerned configuration is as shown in below Fig. 11. The sequence impedance and capacitance values for this configuration is calculated by following the similar steps as described in Section 1.

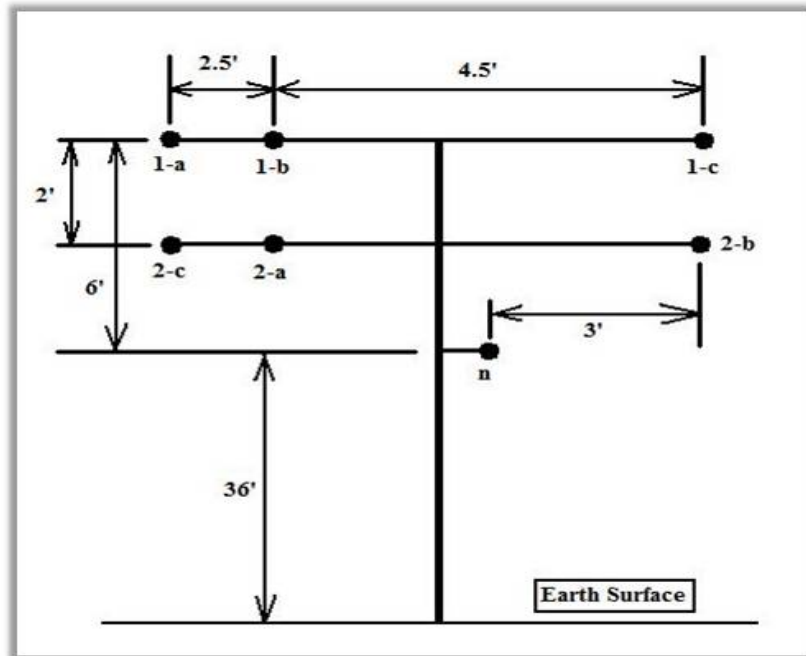


Fig. 11. Three phase double circuit overhead line conductor configuration

The primitive impedance matrix ' Z_{prim} ' for this situation would be of the order [7X7] as observed from the above Fig. 11 [10,11]. Using the Kron reduction formula in Eq 5.5, the primitive impedance matrix is then reduced to a [6X6]

phase impedance matrix ' $Z_{abc,12}$ '. The matrix $Z_{abc,12}$ has the below structure:

$$Z_{abc,12} = \begin{bmatrix} Z_{1a,1a} & Z_{1a,1b} & Z_{1a,1c} & | & Z_{1a,2a} & Z_{1a,2b} & Z_{1a,2c} \\ Z_{1b,1a} & Z_{1b,1b} & Z_{1b,1c} & | & Z_{1b,2a} & Z_{1b,2b} & Z_{1b,2c} \\ Z_{1c,1a} & Z_{1c,1b} & Z_{1c,1c} & | & Z_{1c,2a} & Z_{1c,2b} & Z_{1c,2c} \\ - & - & - & + & - & - & - \\ Z_{2a,1a} & Z_{2a,1b} & Z_{2a,1c} & | & Z_{2a,2a} & Z_{2a,2b} & Z_{2a,2c} \\ Z_{2b,1a} & Z_{2b,1b} & Z_{2b,1c} & | & Z_{2b,2a} & Z_{2b,2b} & Z_{2b,2c} \\ Z_{2c,1a} & Z_{2c,1b} & Z_{2c,1c} & | & Z_{2c,2a} & Z_{2c,2b} & Z_{2c,2c} \end{bmatrix} \quad (5.14)$$

The matrix $Z_{abc,12}$ is then partitioned into four [3X3] matrices as shown in Eq 5.14 . The phase impedance matrix of line 1 in Fig. 11 is obtained by the partitioning of the first three rows and columns, while the phase impedance matrix for line 2 is obtained by the partitioning of the last three rows and columns. The mutual coupling between the two lines is represented by the other two partitioned matrices [12]. To the given line the sequence impedance components is obtained by performing a sequence impedance transformation on the partitioned phase impedance matrix corresponding to that line, as given in equations 5.6 , 5.7. In the similar way for calculating the sequence capacitance values for the configuration of Fig. 11, we first form the [7X7] potential coefficient matrix ' P_{pot} ' as mentioned in Section 1. Using the Kron reduction formula in Eq 5.5, the matrix P_{pot} is then reduced to a [6X6] matrix ' $P_{red,12}$ '. Thereafter, the capacitance matrix ' $C_{red,12}$ ' is obtained by inverting the matrix $P_{red,12}$. Thus, $C_{red,12} = [P_{red,12}]^{-1}$ (nF/km). The [6X6] capacitance matrix $C_{red,12}$ is then partitioned in order to yield four [3X3] matrices. By performing a sequence admittance transformation on the [3X3] capacitance matrix corresponding to

Table VI. Sequence impedance and capacitance values for three phase double circuit overhead line

| | Conductor Size | $Z_1(\Omega/\text{km})$ | $Z_0(\Omega/\text{Km})$ | $C_1(\text{nF}/\text{Km})$ |
|--------|----------------|-------------------------|-------------------------|----------------------------|
| Line 1 | 397.5 kcmil | $0.1752 + j * 0.3948$ | $0.3532 + j * 1.1693$ | 11.7681 |
| Line 2 | 266.8 kcmil | $0.2602 + j * 4138$ | $0.4475 + j * 1.1187$ | 11.2772 |

the concerned line, the sequence capacitance values associated with each line of Fig. 11 are obtained [8,12]. The below table VI shows the different sequence impedance and capacitance values calculated for the three phase, double circuit overhead lines present in the electrical distribution network of Micropolis.

4. Two phase overhead lines: All the two phase overhead lines of Micropolis are assumed to have the same conductor configuration as that shown in Fig. 12. The primitive impedance matrix for this from the Fig. 12 would be of the order [3X3] as shown below.

$$Z_{prim} = \begin{bmatrix} z_{aa} & z_{ac} & z_{an} \\ z_{ca} & z_{cc} & z_{cn} \\ z_{na} & z_{nc} & z_{nn} \end{bmatrix} \quad (5.15)$$

Using the Kron reduction formula in Eq 5.5, the primitive impedance matrix of Eq 5.15 is then reduced to a [2X2] phase impedance matrix ' Z_{ac} '. The [3X3] 'phase frame' matrix ' Z_{abc} ' is then constructed from Z_{ac} by filling in '0's for the

missing phase as shown below.

$$Z_{abc} = \begin{bmatrix} Z_{aa} & 0 & Z_{ac} \\ 0 & 0 & 0 \\ Z_{ca} & 0 & Z_{cc} \end{bmatrix} \quad (5.16)$$

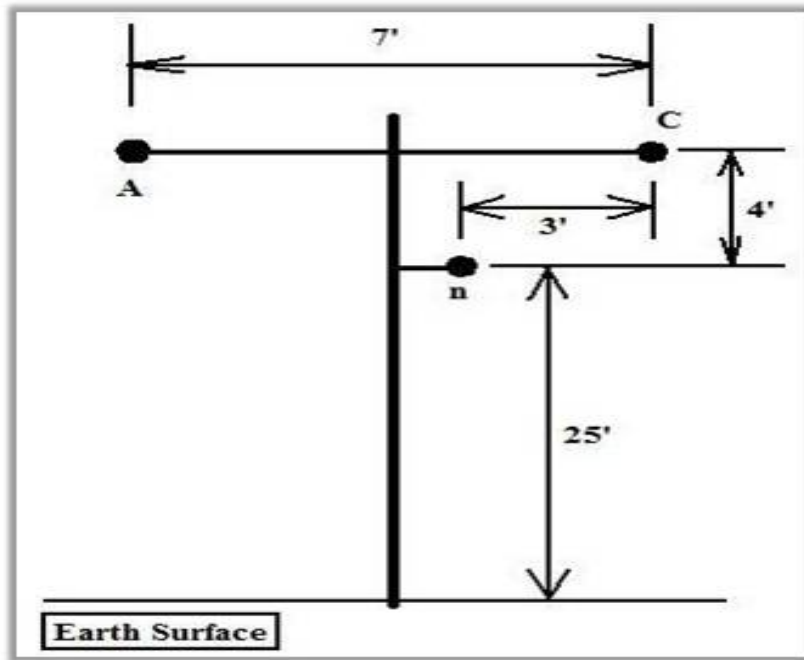


Fig. 12. Two phase overhead line conductor configuration

By performing a sequence impedance transformation on Z_{abc} , the sequence impedance components are calculated as explained as given in equations 5.6, 5.7. Corresponding to the configuration of Fig 12, the sequence capacitance terms are calculated by first forming the [3X3] potential coefficient matrix ' P_{pot} '. Using the Kron reduction formula as given in Eq 5.5, the matrix P_{pot} is then reduced to a [2X2] matrix ' $P_{red,ac}$ '. Thereafter the capacitance matrix ' $C_{red,ac}$ ' is obtained by inverting the matrix $P_{red,ac}$. Thus, $C_{red,ac} = [P_{red,ac}]^{-1}$ (nF/km).

The [3X3] ‘phase frame’ matrix ‘ $C_{red,abc}$ ’ is then constructed from $C_{red,ac}$ by filling in ‘0’s for the missing phase as shown below.

$$C_{red,abc} = \begin{bmatrix} C_{aa} & 0 & C_{ac} \\ 0 & 0 & 0 \\ C_{ca} & 0 & C_{cc} \end{bmatrix} \quad (5.17)$$

The sequence capacitance terms are obtained by performing a transformation on $C_{red,abc}$, as explained using Eq 5.12. The sequence impedance and capacitance values for the configuration of Fig 12 are given as:

$$Z_1 = 1.8021 + j * 0.4941 \Omega/\text{km} \text{ and } Z_0 = 1.9263 + j * 0.9011 \Omega/\text{km} \quad (5.18)$$

$$C_1 = 5.0289 \text{ nF}/\text{km} \text{ and } C_0 = 3.7739 \text{ nF}/\text{km} \quad (5.19)$$

From the above calculations, the positive sequence impedance of the line is determined. This value is multiplied with length of the line to obtain the respective impedances. These impedances are defines as weights to build the graph model of Micropolis in matlab [13]. Fig.13 shows the graph with weights as impedances, the reference node and the three normally open switches present in the city.

3. Simulation inputs and outputs

All the simulation inputs discussed for the case without routing are even the inputs for routing algorithm. But in this case, there are some inputs generated in the process of simulation. They are:

1. After all the iterations are done for a particular wind speed, the nodes for the faulted lines are identified and used to build a graph with the updated weights.

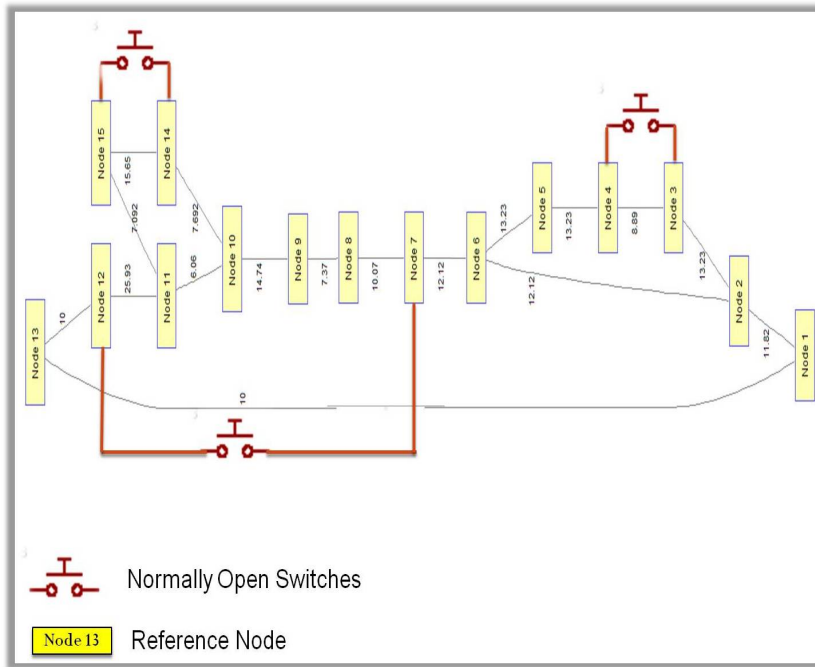


Fig. 13. Graphical representation of Micropolis testbed

2. The nodes holding the normally open switches are also inputs in finding the shortest path.
3. The weights are updated and are used as inputs to find the shortest path.

The outputs are the same as discussed for the case without routing.

B. Results

1. Effect of hurricanes over single family residentials

Fig. 14 shows the fragility curves plotted for both the cases, without routing and with routing. On observation, the number of houses losing power for a particular wind speed is higher in the case without routing. Around a high wind speed of 150 mph, both the curves saturate at one point. At this speed, all the single family residentials in the city are out of power. Confidence interval of 95% is plotted for the

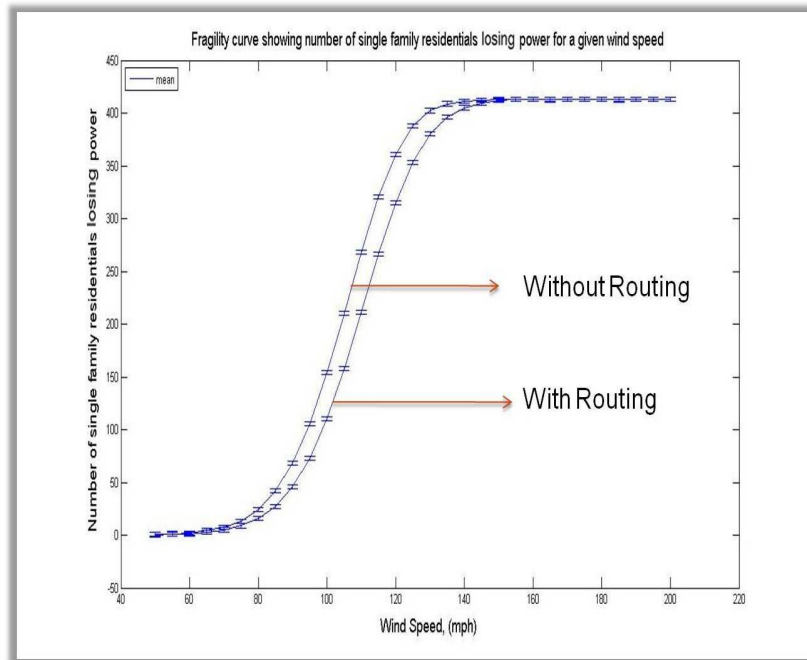


Fig. 14. Fragility curve showing number of single family residential losing power for a range of wind speeds in the presence of routing

fragility curves. The exact number of houses out of power for a particular wind speed in both cases are shown in the table VII. The Fig. 15 emphasizes the importance of power routing by showing the difference in both scenarios (routing and no routing).

2. Effect of hurricanes over multi-family residential

Fig. 16 shows the fragility curves plotted for both the cases, without routing and with routing. On observation, the number of houses losing power for a particular wind speed is higher in the case without routing. Around a high wind speed of 140 mph, both the curves saturate at one point. At this speed, all the multi-family residential in the city are out of power. Confidence interval of 95% is plotted for the fragility curves. The exact number of houses out of power for a particular wind speed in both cases are shown in the table VIII. The Fig. 17 emphasizes the importance of

Table VII. Number of single family residentials losing power vs wind speed

| Wind Speed | Number of single family residentials losing power | |
|------------|---|--------------|
| | Without Routing | With Routing |
| 70 | 8 | 5 |
| 80 | 25 | 15 |
| 90 | 70 | 45 |
| 100 | 156 | 109 |
| 110 | 268 | 211 |
| 120 | 360 | 316 |
| 130 | 402 | 380 |
| 140 | 411 | 405 |
| 150 | 413 | 413 |

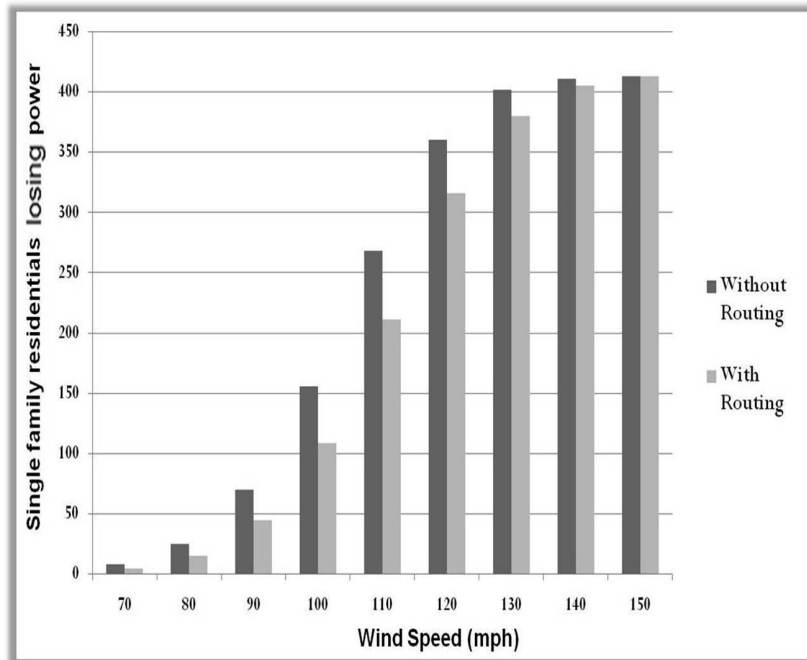


Fig. 15. Bar graph representing the number of single family residences losing power

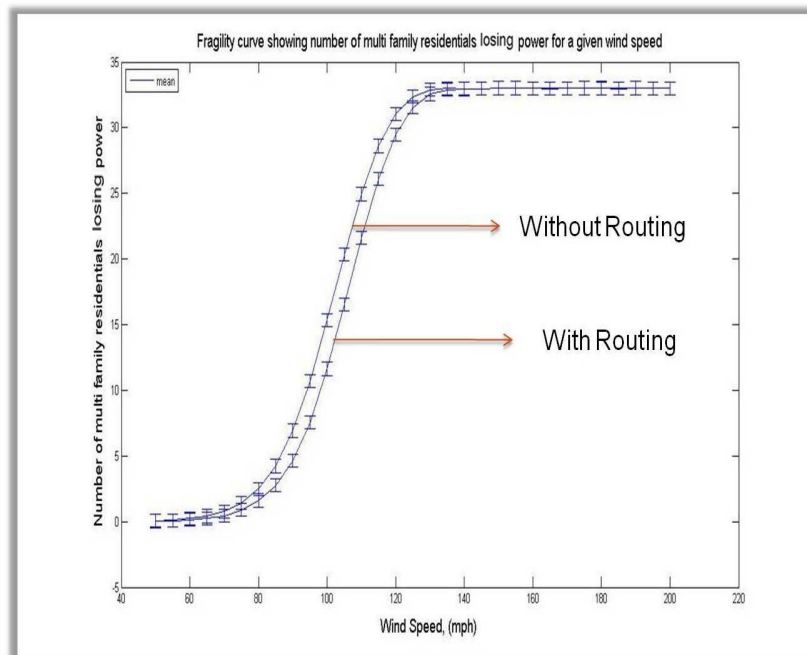


Fig. 16. Fragility curve showing number of multi-family residences losing power for a range of wind speeds in the presence of routing

Table VIII. Number of multi-family residentials losing power vs wind speed

| Wind Speed | Number of multi-family residentials losing power | |
|------------|--|--------------|
| | Without Routing | With Routing |
| 70 | 1 | 1 |
| 80 | 2 | 1 |
| 90 | 7 | 5 |
| 100 | 15 | 11 |
| 110 | 25 | 21 |
| 120 | 31 | 29 |
| 130 | 33 | 32 |
| 140 | 33 | 33 |
| 150 | 33 | 33 |

power routing by showing the difference in both scenarios (routing and no routing).

3. Effect of hurricanes over commercial complexes

Fig. 18 shows the fragility curves plotted for both the cases, without routing and with routing. On observation, the number of houses losing power for a particular wind speed is higher in the case without routing. Around a high wind speed of 160 mph, both the curves saturate at one point. At this speed, all the commercial complexes in the city are out of power. Confidence interval of 95% is plotted for the fragility curves. The exact number of houses out of power for a particular wind speed

Table IX. Number of commercial complexes losing power vs wind speed

| Wind Speed | Number of commercial complexes losing power | |
|------------|---|--------------|
| | Without Routing | With Routing |
| 70 | 1 | 1 |
| 80 | 3 | 1 |
| 90 | 7 | 4 |
| 100 | 16 | 10 |
| 110 | 28 | 21 |
| 120 | 40 | 33 |
| 130 | 45 | 42 |
| 140 | 46 | 45 |
| 150 | 46 | 46 |

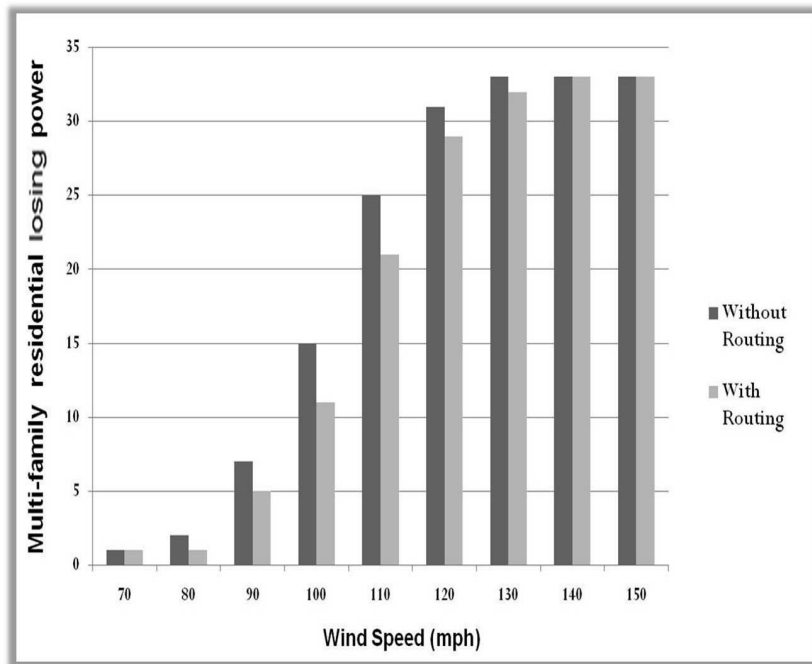


Fig. 17. Bar graph representing number of multi-family residential losing power for a range of wind speeds

in both cases are shown in the table IX. The Fig. 19 emphasizes the importance of power routing by showing the difference in both scenarios (routing and no routing).

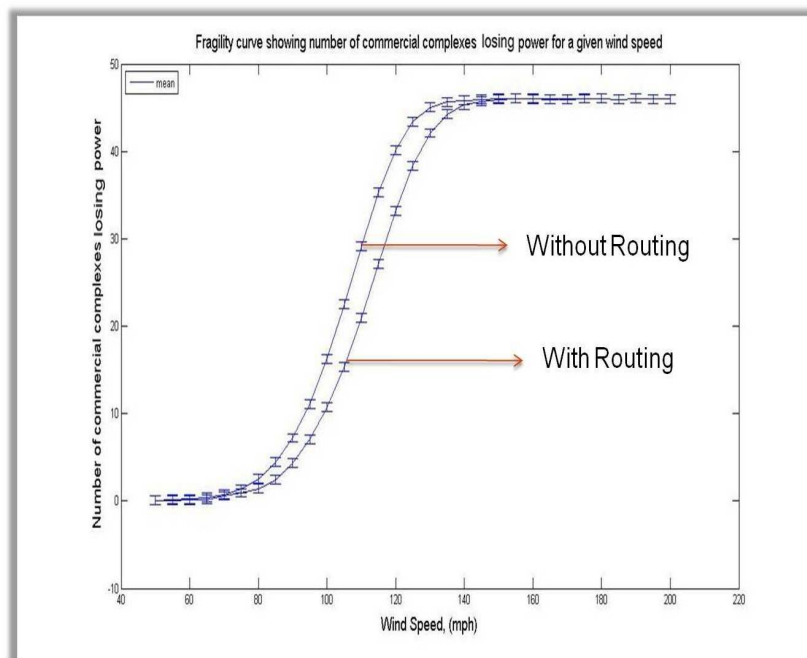


Fig. 18. Fragility curve showing number of commercial complexes losing power for a range of wind speeds in the presence of routing

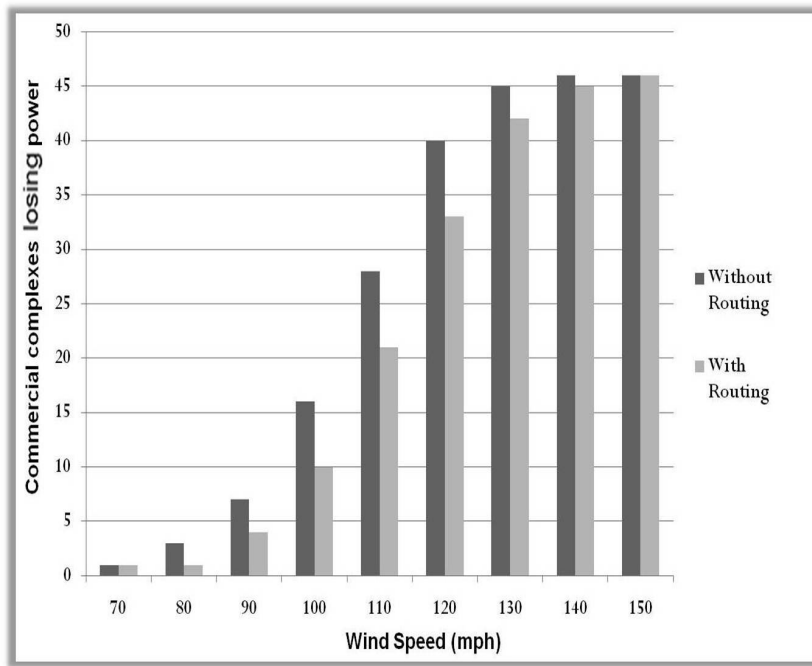


Fig. 19. Bar graph representing number of commercial complexes losing power for a range of wind speeds

CHAPTER VI

MULTISCALE APPROACH

In this chapter, we discuss a multiscale approach to estimate the effects of hurricanes over a large area. A large testbed, Mesopolis was developed using GIS (ArcMap) and hydraulic modeling (EPANet) based software. Fragility based analysis is done over a small area and later extrapolated for similar areas throughout the Mesopolis. Mesopolis is categorized into areas called the test zones like light residential zone, medium residential zone, etc. Fragility curves are obtained for these test zones and are used to estimate the power outages for the rest of the city. For instance, fragility curve obtained from the completed light residential test zone is used to estimate the number of houses lost in all the other light residential zones. These curves estimate the percentage of damage for a particular wind speed throughout the city. This lays a great platform for researchers to analyze the effects in a detailed way. Some of the features of Mesopolis are:

1. A power generating station located in its vicinity supplies power to the city where as there is no power plant in Micropolis.
2. Population of the city is around 140,000 residents and is spread over a very large area.
3. From the infrastructural point of view, Mesopolis is very advanced as it has huge constructions like airport, naval base, university etc.
4. Depending on the number of people living in a given area, whole of Mesopolis is broadly classified into Residential low, Residential medium and Residential regions.

5. Depending on the number of commercial complexes in a given area, whole of Mesopolis is broadly classified into commercial low, commercial medium and commercial high regions.
6. Depending on the number of industries in a given area, whole of Mesopolis is broadly classified into industrial low, industrial medium and industrial high regions.
7. It has been elaborately designed with freeways, roads, streams etc., embedded in the testbed.
8. Electrical distribution system of Mesopolis can be prohibitively large. Unlike Micropolis, in this case there are a couple of substations at strategic positions all over the Mesopolis. Presently a portion of Mesopolis has been supported by electrical distribution system. This proved to be a great platform to analyze the effects on this portion and then to estimate the effects on similar regions throughout Mesopolis. In future, once Mesopolis is complete, it becomes a useful testbed to observe adverse effects of natural disasters in a more realistic way [3].

A. Layout of Mesopolis

1. Infrastructure components layout

Fig. 20 shows Mesopolis having one generating station (covered in the figure by an inter-city tie line) around 8 substations to supply power for the entire area [14,15]. It shows various small zones in different colors which are categorized depending on the density of population in that particular zone. It also shows a transmission loop and also some distribution feeders which have been incorporated in the testbed after

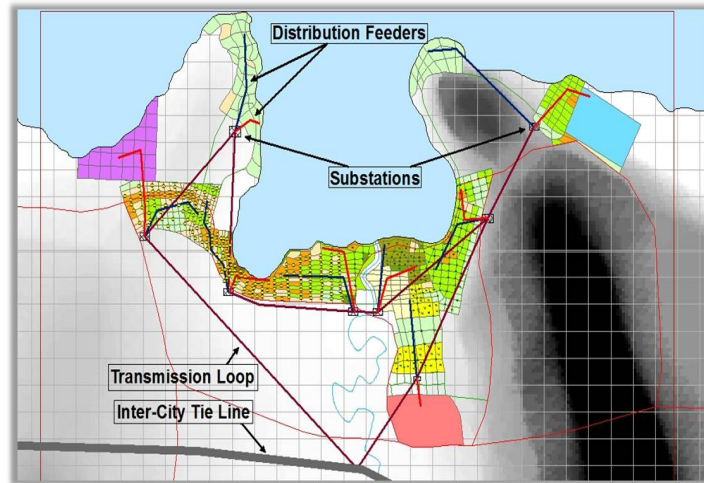


Fig. 20. Mesopolis overview

discussion with college station utilities. Detailed explanation of areas are presented in the next section.

2. Different layers of Mesopolis

In this section, different layers of Mesopolis are shown which give complete information regarding the testbed. The Fig. 21 labels different zones in the Mesopolis depending on the factors like population density, infrastructure components etc. The table X shows the assumed KVA ratings used for different zones and also determines the transformer ratings depending on these assumptions. Figures 22 and 23 shows the freeways, streams, pressurezones etc. in the city.

B. Area Considered for Study

A portion of Mesopolis is considered for analysis. The table XI shows the number of light and medium residentials present in the considered area. This focused area has a small distribution system that could supply the entire area. There is one main feeder

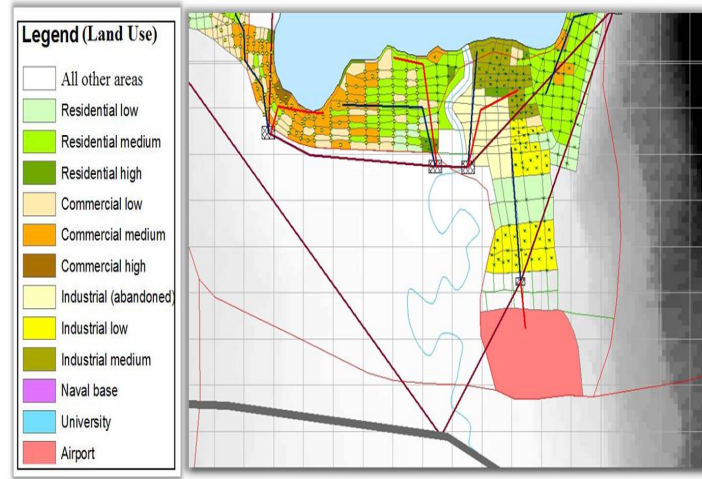


Fig. 21. Mesopolis infrastructure layout

Table X. Assumed average KVA consumption and transformer ratings for different zones

| Zone Type | KVA | Units per transformer | Rating (KVA) |
|-----------|-----|-----------------------|--------------|
| Res Low | 5 | 4 | 25 |
| Res Med | 4 | 5 | 25 |
| Res High | 3 | 4 | 15 |
| Comm Low | 10 | 4 | 50 |
| Comm Med | 9 | 4 | 50 |
| Comm High | 8 | 5 | 50 |
| Ind Low | 100 | 1 | 167 |
| Ind Med | 90 | 1 | 167 |
| Ind High | 80 | 1 | 100 |



Fig. 22. Mesopolis roads and freeways layout

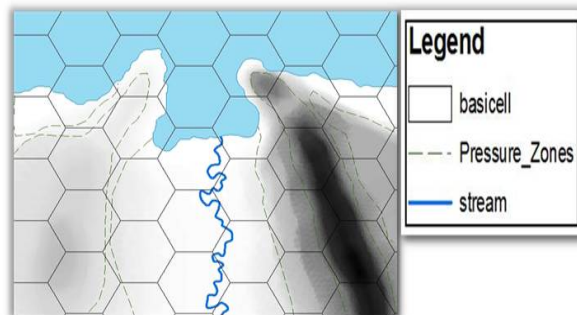


Fig. 23. Mesopolis pressure zones

Table XI. Total light and medium residential in the focused area

| | Light Residential | Medium Residential |
|------------------------|--------------------------|---------------------------|
| Total Number of Houses | 522 | 2484 |

which branches off into 6 lines and then these split into several laterals which feed the consumers. The electrical distribution system is explained later in this section.

1. Overview of the focused area

Fig. 24 shows the area under consideration. The area used to calculate the fragility curves is encircled by the purple line seen on the right. It should be noted, however, that the fragility curves were only calculated for the medium residential (green in color) and light residential (light green in color).

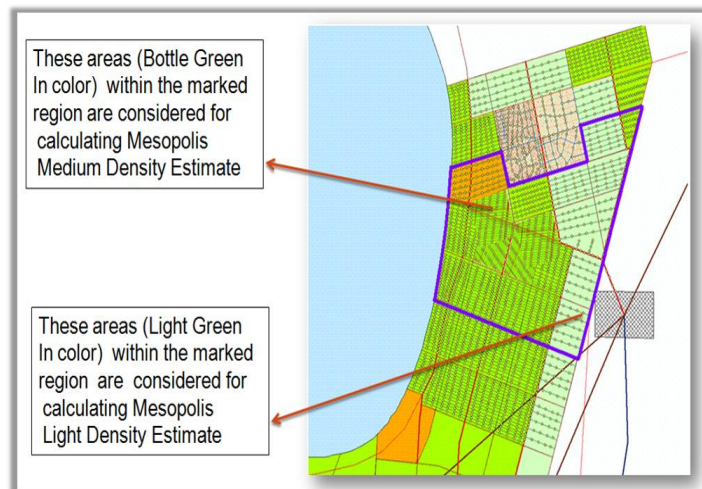


Fig. 24. Focused area of Mesopolis

2. Electrical distribution system for focused area

Fig. 25 shows the electrical distribution system for area under consideration. Based on the table X, average consumption of light residentials in the area is 2610 KVA and medium residentials is 9936 KVA. There are about 223 laterals in the system [15]. The red arrow marks indicate the direction of current.

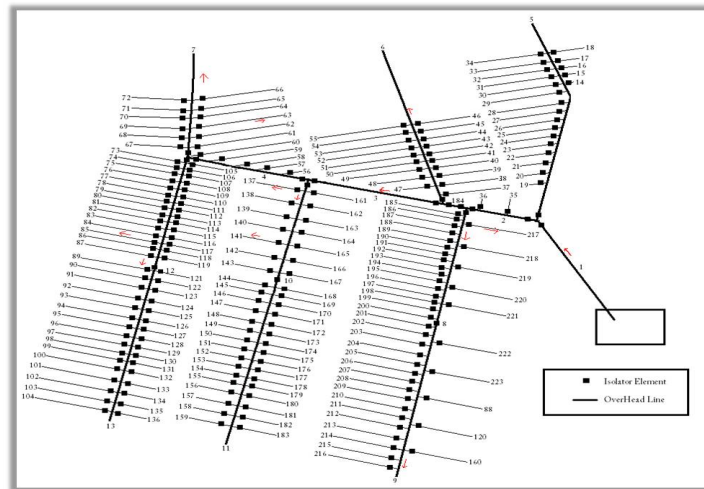


Fig. 25. Electrical distribution system for considered area of Mesopolis

C. Results

1. Fragility curves showing number of light and medium areas out of power

Figures 26 and 27 show the fragility curves determining the number of light residentials and medium residentials are out of power for a given wind speed respectively. On observation, the number of houses losing power increases along with the wind speed. Around a high wind speed of 150 mph, the curve saturates. At this wind speed, all the single family residentials in the city are out of power. Confidence interval of 95% is plotted for the fragility curves. This shows that for wind speeds of 140 mph and above total single family residentials will be out of power.

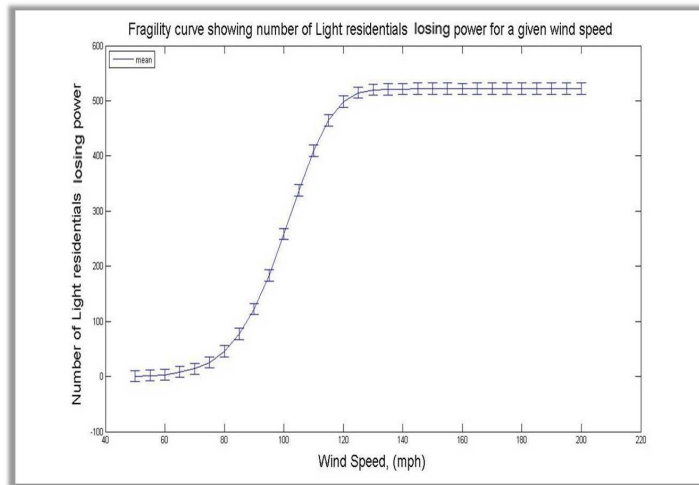


Fig. 26. Fragility curves showing number of light and medium areas out of power for a given wind speed

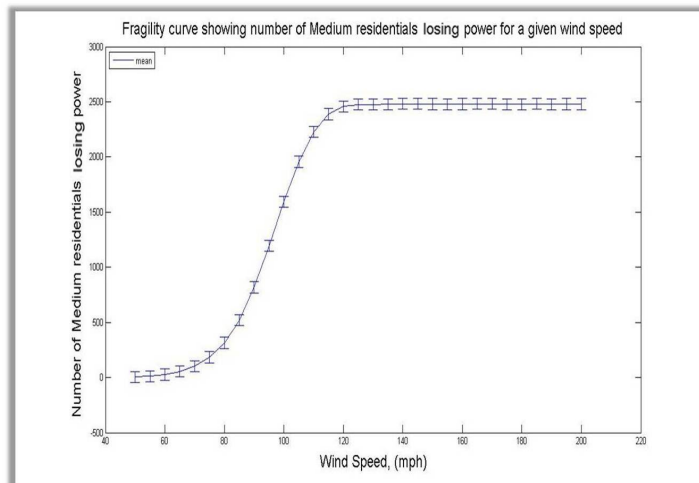


Fig. 27. Fragility Curves showing number of medium areas out of power for a given wind speed

2. Comparison of effect of hurricanes over Mesopolis and Micropolis

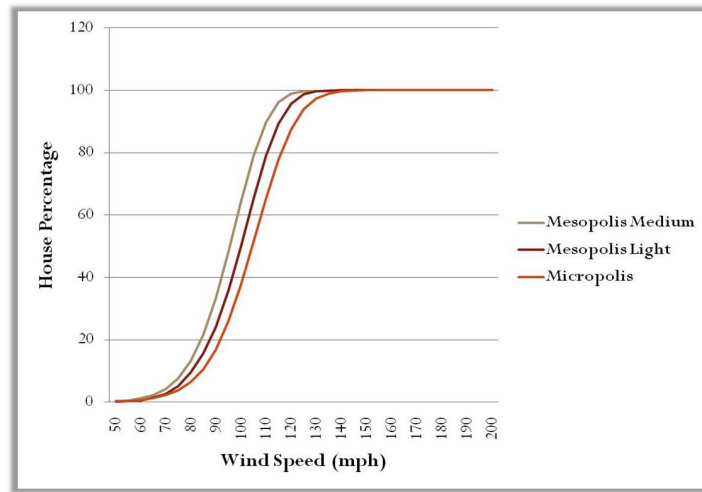


Fig. 28. Comparison of effect of hurricanes over Mesopolis and Micropolis

Fig. 28 gives the information of the percentage of houses losing power for a wind speed range of 50 to 200 mph. From the figure, one can observe that the medium and light density residential areas have high percentage of houses losing power compared to Micropolis. Main reason for this is the number of houses present in each of them. For the focused area of Mesopolis, medium density residentials are 2484 and light residentials are 522 while the residentials in Micropolis are 413. Also, in Micropolis as shown in fig. 3 there are two feeders that supply power to the city. But in case of focused area of Mesopolis (as shown in fig. 25), only one feeder is present. The probability of this feeder going down is high compared to two feeders in earlier case. The table XII shows the number of light residentials and house percentage losing power for a given wind speed. It also shows normalized values for a given wind speed. Table XIII shows the number of medium residentials and house percentage losing power for a given wind speed. It also shows normalized values for a given wind speed [14]. Table XIV shows the number of single family residentials out of power and

Table XII. Mesopolis light residential normalized calculations

| Wind | Houses | House Percentage | Normalized |
|------|--------|------------------|-------------|
| 50 | 0.99 | 0.189655172 | 78.51724138 |
| 60 | 2.757 | 0.52816092 | 218.6586207 |
| 70 | 13.86 | 2.655172414 | 1099.241379 |
| 80 | 49.72 | 9.524904215 | 3943.310345 |
| 90 | 125.8 | 24.09961686 | 9977.241379 |
| 100 | 260.5 | 49.90421456 | 20660.34483 |
| 110 | 412.4 | 79.00383142 | 32707.58621 |
| 115 | 466.8 | 89.42528736 | 37022.06897 |
| 120 | 499.9 | 95.76628352 | 39647.24138 |
| 125 | 515.3 | 98.7164751 | 40868.62069 |
| 130 | 520.2 | 99.65517241 | 41257.24138 |
| 135 | 521.4 | 99.88505747 | 41352.41379 |
| 140 | 522 | 100 | 41400 |
| 145 | 522 | 100 | 41400 |

Table XIII. Mesopolis medium residential normalized calculations

| Wind | Houses | House Percentage | Normalized |
|------|--------|------------------|------------|
| 50 | 9.674 | 0.389452496 | 161.23 |
| 60 | 31.88 | 1.283413849 | 531.33 |
| 70 | 101.5 | 4.086151369 | 1691.67 |
| 80 | 328.3 | 13.21658615 | 5471.67 |
| 90 | 827.2 | 33.30112721 | 13786.67 |
| 100 | 1594 | 64.17069243 | 26566.67 |
| 110 | 2229 | 89.73429952 | 37150.00 |
| 115 | 2390 | 96.215781 | 39833.33 |
| 120 | 2458 | 98.95330113 | 40966.67 |
| 125 | 2474 | 99.59742351 | 41233.33 |
| 130 | 2474 | 99.59742351 | 41233.33 |
| 135 | 2478 | 99.75845411 | 41300.00 |
| 140 | 2483 | 99.95974235 | 41383.33 |
| 145 | 2484 | 100 | 41400.00 |

percentage of houses losing power for a given wind speed.

3. Estimated fragility curves for light and medium areas throughout Mesopolis

As seen in Fig. 25, poles/distribution lines are placed in only light residential and medium residential zones of the focused area. These will be called the ‘test zones’. The fragility curves for these test zones are obtained in the previous section (as shown in figures 26 and 27). These specific fragility curves are to estimate the power outages for identical zones in the rest of the city. Fig. 29 shows a hurricane of 180 mph speed originating in zone1 and its speed in different areas considered in a circular fashion [1]. From the specific fragility curves generated for the test zones, we determined the percentage of light and medium residential losing power for a given wind speed. Thus one can estimate the impact of hurricane of a known wind speed over an area similar to the test zones under consideration. Figures 31 and 30 show the percentage of

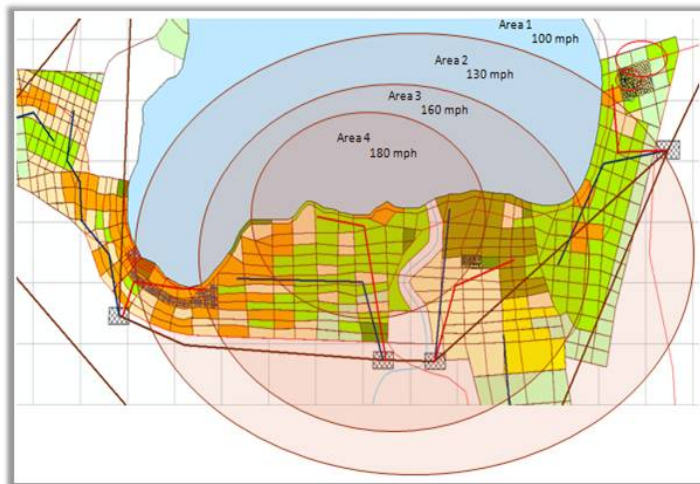


Fig. 29. Varying hurricane wind speeds for different areas of the city

houses losing power for a known wind speed respectively. These give a rough estimate of damage caused to light and medium residential areas through out the city exposed

Table XIV. Micropolis single family residential normalized calculations

| Wind | Houses | House Percentage |
|------|--------|------------------|
| 50 | 1.202 | 0.290338164 |
| 60 | 2.809 | 0.678502415 |
| 70 | 9.418 | 2.274879227 |
| 80 | 26.62 | 6.429951691 |
| 90 | 69.88 | 16.87922705 |
| 100 | 155.8 | 37.63285024 |
| 110 | 270.3 | 65.28985507 |
| 115 | 322.2 | 77.82608696 |
| 120 | 362.4 | 87.53623188 |
| 125 | 388.7 | 93.88888889 |
| 130 | 403.2 | 97.39130435 |
| 135 | 409.8 | 98.98550725 |
| 140 | 412.5 | 99.63768116 |
| 145 | 413.6 | 99.90338164 |

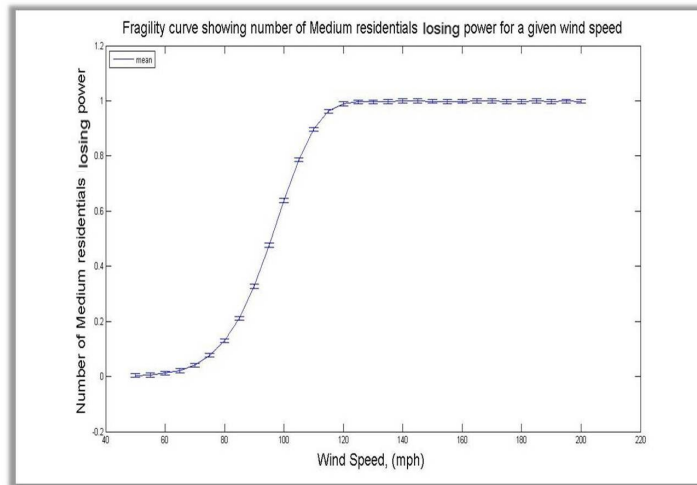


Fig. 30. Fragility curve showing percentage of medium residential losing power for a given wind speed

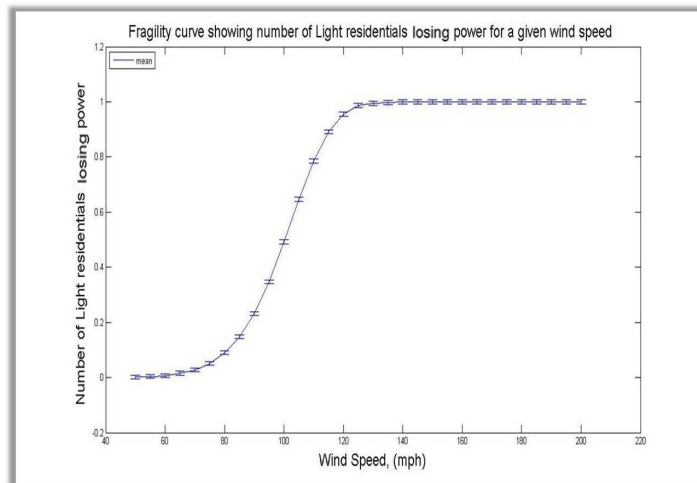


Fig. 31. Fragility curve showing percentage of light residential losing power for a given wind speed

to different hurricane wind speeds.

CHAPTER VII

DETAILED ENGINEERING MODEL

A detailed engineering model is developed using Power World Simulator [5]. It is designed with all the voltage and power ratings as specified in the electrical distribution model of Micropolis [14.15] (shown in Fig. 3). In this thesis, the results obtained by simulating the two models are compared and analyzed. This gives a scope to find the intricacies in both the models so that effective measures can be taken to ensure the accuracy in further studies. It also showcases the correctness of assumptions made and their effects over the end results. Power World Simulator is an extremely visual, power system simulation and analysis package. Simulator has the power for engineering analysis and is interactive and graphical that can be used to explain the power system operation to technical and non-technical audiences. Simulator also provides a convenient medium for simulating the evolution of power system over time. Load, generation, and interchange schedule over time may be prescribed and the resulting change in the system can be visualized. Power world binary (PWB) is the most preferred file type providing the most comprehensive power system information along with the smallest time and quickest load time. Information stored in this format includes power flow data, economic parameters, case time variation, options/values, and screen customization. For interchange of data with other packages auxiliary files are used. They store additional power flow information that is not contained in power flow data files and do not have .pwb format. The format of an auxiliary file and its importance are discussed later in the thesis [5].

A. Micropolis Engineering Model

Based on the calculations done in Chapter IV, the voltage and power ratings are used to develop the engineering model. The main features of this model are:

1. The two feeders from the substation are treated as two generators.
2. One of the generator bus is treated as a slack bus which also accounts for losses in the system.
3. There are around 38 buses throughout the distribution system.
4. All the distribution lines are designated with impedance values calculated in Chapter IV.
5. Each line in the electrical distribution system of Micropolis is replaced by a bus and the load at the bus corresponds to that line.
6. Each load has active and reactive power variables assigned which allow the load increments or decrements to be done at a particular bus.
7. The simulator options are set as follows;
 - (a) Convergence tolerance is set to 0.1.
 - (b) Maximum number of iterations is set to 100.
 - (c) Assumed 100.00 MVA per unit base.
 - (d) Solution method set is power flow analysis.
 - (e) The limits are set such that the overloaded lines are automatically opened.
 - (f) File management is set such that an auxiliary file generated is automatically loaded when the present case is opened.

- (g) The limit monitoring settings are set with percentage of voltage allowed at a bus as minimum and maximum.
- (h) Only one default limit group is defined.

The engineering model in power world is as shown in Fig. 32.

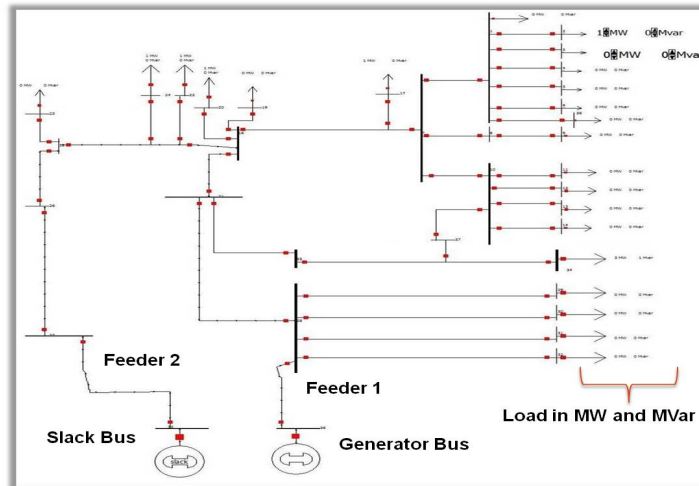


Fig. 32. Micropolis power world model

B. Power World and Matlab Interaction

As discussed earlier, for interchange of data with other packages auxiliary files are used. They store additional power flow information that is not contained in power flow data files and do not have .pwb format. The data can be stored and edited in a text file format. There are two types of auxiliary files:

1. Data auxiliary file (.aux) : This file generally contains the power flow information. In this research, an algorithm written in matlab generates this file for different wind speeds. It contains the details of all faulted buses. This file is automatically loaded in the power world and with the updated system, a set of iterations are run until the convergence is reached.

2. Display auxiliary file (.axd) : There are separate files called display auxiliary files that are available for importing display data to/from Simulator in a text format.

There are two sections in an auxiliary file, script section and data section. A data section provides specific data for a specific type of object. A script section provides a list of script actions for simulator to perform. Simulator actually uses three nested loops to solve the power flow. They are:

1. MW control loop
2. Voltage controller loop
3. Inner power flow loop

We used Gauss Seidel method for the inner power flow loop. Gauss Seidel method is discussed briefly in the next paragraph.

1. Gauss Seidel method

Consider a typical bus as shown in Fig. 33. Applying Kirchoff's current laws to this bus results in [14,15]

$$\begin{aligned} I_i &= y_{i0}V_i + y_{i1}(V_i - V_1) + y_{i2}(V_i - V_2) + \dots + y_{in}(V_i - V_n) \\ &= (y_{i0} + y_{i1} + y_{i2} + \dots + y_{in})V_i - y_{i1}V_1 - y_{i2}V_2 - \dots - y_{in}V_n \end{aligned} \quad (7.1)$$

$$I_i = V_i \sum_{j=0}^n y_{ij} - V_i \sum_{j=1}^n y_{ij} V_j \quad j \neq i \quad (7.2)$$

The real and reactive power at bus i is

$$P_i + jQ_i = V_i I_i^* \quad (7.3)$$

$$I_i = \frac{P_i - jQ_i}{V_i^*} \quad (7.4)$$

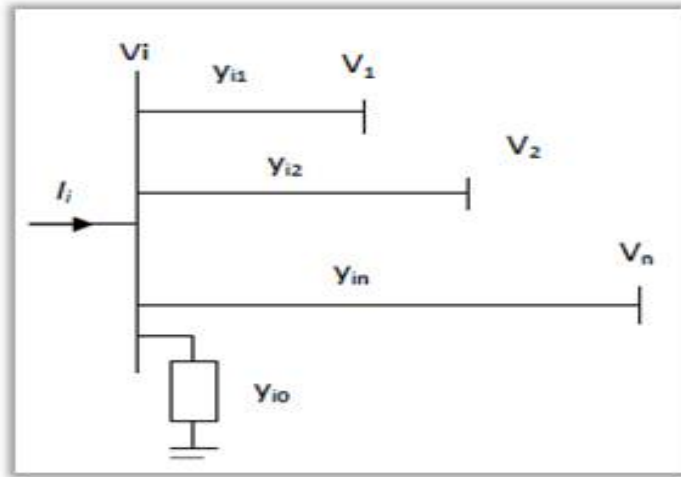


Fig. 33. Example of a typical bus in a power system

Substituting for I_i in Eq (7.2) yields

$$\frac{P_i - jQ_i}{V_i^*} = V_i \sum_{j=0}^n y_{ij} - V_i \sum_{j=1}^n y_{ij} V_j \quad j \neq i \quad (7.5)$$

Equation (7.5) is an algebraic non linear equation which must be solved by iterative techniques.

Equation (7.5) is solved for V_i iteratively

$$V_i^{(k+1)} = \frac{\frac{P_i^{sch} - jQ_i^{sch}}{V_i^{*(k)}} + \sum y_{ij} V_j^{(k)}}{\sum y_{ij}} \quad j \neq i \quad (7.6)$$

where y_{ij} is the actual admittance in *p.u.*

P_i^{sch} and Q_i^{sch} are the net real and reactive powers in *p.u.*

In writing the KCL, current entering bus I was assumed positive. Thus for :

Generator buses (where real and reactive powers are injected), P_i^{sch} and Q_i^{sch} have positive values.

Load buses (real and reactive powers flow away from the bus), P_i^{sch} and Q_i^{sch} have negative values.

Equation (7.5) can be solved for P_i and Q_i

$$P_i^{(k+1)} = R\{V_i^{*(k)} \left[V_i^{(k)} \sum_{j=0}^n y_{ij} - \sum_{j=1}^n y_{ij} V_j^{(k)} \right]\} j \neq i \quad (7.7)$$

$$Q_i^{(k+1)} = -Im\{V_i^{*(k)} \left[V_i^{(k)} \sum_{j=0}^n y_{ij} - \sum_{j=1}^n y_{ij} V_j^{(k)} \right]\} j \neq i \quad (7.8)$$

The power flow equation is usually expressed in terms of the elements of the bus admittance matrix, Y_{bus} , shown by upper case letters, are $Y_{ij} = -y_{ij}$, and the diagonal elements are $Y_{ii} = \sum y_{ij}$. Hence Equation (7.6) can be written as

$$V_i^{(k+1)} = \frac{\frac{P_i^{sch} - jQ_i^{sch}}{V_i^{*(k)}} + \sum_{j \neq i} Y_{ij} V_j^{(k)}}{Y_{ii}} j \neq i \quad (7.9)$$

$$P_i^{(k+1)} = R\{V_i^{*(k)} \left[V_i^{(k)} Y_{ii} + \sum_{j=1, j \neq i}^n Y_{ij} V_j^{(k)} \right]\} j \neq i$$

$$Q_i^{(k+1)} = -Im\{V_i^{*(k)} \left[V_i^{(k)} Y_{ii} + \sum_{j=1, j \neq i}^n Y_{ij} V_j^{(k)} \right]\} j \neq i$$

Iterativesteps :

1. Slack bus: both components of the voltage are specified. $2(n-1)$ equations to be solved iteratively.
2. Flat voltage start: initial voltage of $1.0+j0$ for unknown voltages.

3. PQ buses: P_i^{sch} and Q_i^{sch} are known. with flat voltage start, Eqn.(7.9) is solved for real and imaginary components of Voltage.
4. PV buses: P_i^{sch} and $[V_i]$ are known. Eqn.(7.11) is solved for Q_i^{k+1} which is then substituted in Eqn.(7.9) to solve for V_i^{k+1}

However, since $[V_i]$ is specified, only the imaginary part of V_i^{k+1} is retained, and its real part is selected in order to satisfy

$$(e_i^{(k+1)})^2 + (f_i^{(k+1)})^2 = |V_i|^2 \quad (7.12)$$

or

$$e_i^{(k+1)} = \sqrt{|V_i|^2 - (f_i^{(k+1)})^2} \quad (7.13)$$

These equations are used to determine voltages at all the buses in the system and checked whether they are in the limits. The voltage at the bus which violates the constraints becomes zero and the power flow analysis is done with the updated values till convergence is reached.

C. Results

1. Comparison between engineering model and connectivity based model
 - a. Voltage constraint at a bus is set to 5 percent of nominal voltage

In this case, only 5% of the nominal voltage is set as the limits at each bus [5]. Violation of these limits will make the voltage at that bus as zero and the power flow is run till the convergence is reached. The Fig. 34 shows the fragility curves plotted

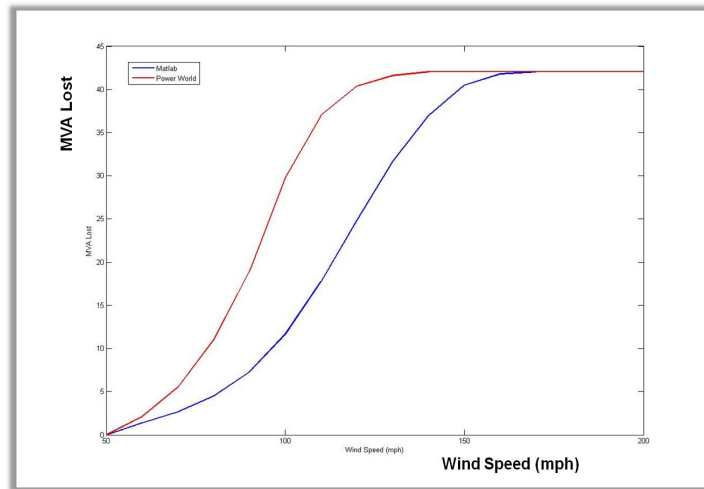


Fig. 34. Comparison of results from matlab and power world when voltage change allowed is 10% of nominal

based on results from both the models, connectivity based model and engineering based model. On observation, the MVA lost for a particular wind speed is higher in the case of engineering model. The comparison of MVA lost for all the wind speeds in both the models is shown by the table a. The engineering model based fragility curve saturates around a wind speed of 130 mph where as the connectivity model fragility curve saturates around 160 mph. This shows the exact electrical behaviour of the system which is more closer to a real time scenario.

b. Voltage constraint at a bus is set to 10 percent of nominal voltage

In this case, only 10% of the nominal voltage is set as the limits at each bus. Violation of these limits will make the voltage at that bus as zero and the power flow is run till the convergence is reached. The Fig. 35 shows the fragility curves plotted based on results from both the models, connectivity based model and engineering based model. On observation, the MVA lost for a particular wind speed is higher in the case of engineering model. The comparison of MVA lost for all the wind speeds in

Table XV. When the voltage constraints at a bus are 5% of nominal voltage

| Wind Speed | MVA lost - matlab | MVA lost - power world |
|------------|-------------------|------------------------|
| 50 | 0 | 0 |
| 60 | 1.393 | 2.12 |
| 70 | 2.659 | 5.5 |
| 80 | 4.499 | 11 |
| 90 | 7.275 | 19 |
| 100 | 11.65 | 29.8 |
| 110 | 17.76 | 37 |
| 120 | 24.870 | 40.38 |
| 130 | 31.67 | 41.6 |
| 140 | 40.5 | 42.030 |
| 150 | 41.8 | 42.03 |
| 160 | 42.03 | 42.03 |
| 170 | 42.03 | 42.03 |
| 180 | 42.03 | 42.03 |
| 190 | 42.03 | 42.03 |
| 200 | 42.03 | 42.03 |

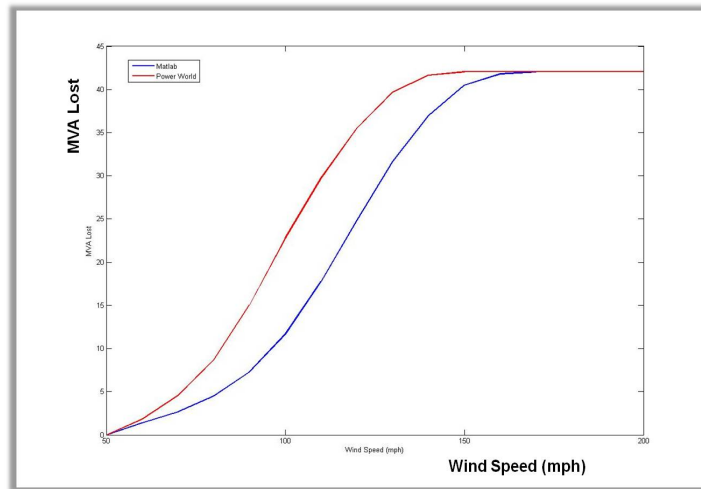


Fig. 35. Comparison of results from matlab and power world when voltage change allowed is 10% of nominal

both the models is shown by the table XVI. The engineering model based fragility curve saturates around a wind speed of 145 mph whereas the connectivity model fragility curve saturates around 160 mph. In comparison with the case considered in the previous section (where 5% of voltage change is allowed), the MVA lost in present case is low for a particular wind speed. We can say that as the voltage variations of wide range are accepted, the system tends to be more stable but in real time large voltage variations are unacceptable as they may damage costly electrical equipments.

Table XVI. When the voltage constraints at a bus are 10% of nominal voltage

| Wind Speed | MVA lost - matlab | MVA lost - power world |
|-------------------|--------------------------|-------------------------------|
| 50 | 0 | 0 |
| 60 | 1.39 | 1.8 |
| 70 | 2.657 | 4.56 |
| 80 | 4.496 | 8.65 |
| 90 | 7.273 | 15.03 |
| 100 | 11.65 | 22.78 |
| 110 | 17.76 | 29.723 |
| 120 | 24.87 | 35.54 |
| 130 | 31.67 | 39.68 |
| 140 | 40.5 | 41.65 |
| 150 | 41.8 | 42.03 |
| 160 | 42.03 | 42.03 |
| 170 | 42.03 | 42.03 |
| 180 | 42.03 | 42.03 |
| 190 | 42.03 | 42.03 |
| 200 | 42.03 | 42.03 |

CHAPTER VIII

CONCLUSION

Main purpose of this thesis is to develop an efficient methodology for estimating the impact of hurricanes on small and large cities. It aims to estimate the impact of power re-routing for reliability estimation. It also compares engineering and connectivity based models. Finally, to validate these concepts it aims at develop synthetic cities. The research work done can give useful insights like:

1. It was feasible to efficiently run the re-routing algorithm to supply power to maximum possible faulted sections of the city.
 - (a) Through power re-routing, help and search operations can be extracted to the maximum.
2. The comparison between engineering model and connectivity-based model suggested the intricacies in the connectivity-based model like:
 - (a) Electrical structure of system is not considered.
 - (b) No power flow is accounted.
 - (c) Transients are not captured in a better way.
3. A virtual city developed gives more space of research and produces reliable and accurate results.
4. Serve as a platform for future research in applying the methodologies to analyze the severity of the situation and help safety personnel to take pre-storm precautions.

This work would be a platform for future research in applying the methodologies to analyze the severity of the situation and helpful for safety personnel for taking pre-storm precautions. Some of the directions of future research are as follows:

1. Examine effects of power system failures on other infrastructure like water, communications, etc.
2. Analyze the resilience of a city with real hurricane data.
3. Calculate several reliability indices.
4. Propose optimization algorithms.

REFERENCES

- [1] S. R. Han, S. D. Guikema, S. M. Quiring, “Improving the predictive accuracy of hurricane power outage forecasts using generalized additive models”, *Risk Analysis*, Vol. 29, no. 10, 2009.
- [2] Hurricane website. [Online]. Available: <http://www.wunderground.com/hurricane>. Accessed: March 28, 2011.
- [3] K. Brumbelow, J. Torres, S. Guikema, E. Bristow, and L. Kanta, “Virtual cities for water distribution and infrastructure system research”, in Proceedings of the World Environmental and Water Resources Congress, May 2007.
- [4] K. Jones and I. Horbaczewski, “Micropolis: A power distribution system for a virtual city for research applications”, Undergraduate research report, Texas A&M University, College Station, TX, Mar. 2008.
- [5] Power World website. [Online]. Available: <http://www.powerworld.com/products>. Accessed: March 25, 2010.
- [6] J. Winkler, L. Duen-asosri, R. Stein, D. Subramanian, “Performance assessment of topologically diverse power systems subjected to hurricane events”, *Reliability Engineering and System Safety*, Vol. 95, 2010.
- [7] C. Singh, A. Bagchi, “Reliability analysis of power systems incorporating renewable energy sources”. Presented at 16th National Power Systems Conference, Hyderabad, India, December 2010.
- [8] B. Adkins, R.G. Harley, *The General Theory of Alternating Current Machines*, NY: Routledge, Chapman & Hall, Incorporated, 1975.

- [9] P. H. Smith, “Electrical distribution modeling: an integration of engineering analysis and geographic information systems”, M.S. thesis, Virginia Polytechnic Institute and State University, 2007.
- [10] J.D. Glover, M.S. Sarma and T.J. Overbye, *Power System Analysis and Design*, Toronto, Canada: Thomson Learning, 2008.
- [11] H.W. Beaty, *Handbook of Electric Power Calculations*, NY: McGraw-Hill, 2001.
- [12] T.H. Chen, S.W. Wang, “Simplified three-phase lateral and feeder models for fast distribution system calculations”, *Electric power systems research*, Vol. 39, no. 1, 1996.
- [13] N. Deo, *Graph Theory with Applications to Engineering and Computer Science*, Englewood Cliffs, NJ, Prentice-Hall Inc., 1974.
- [14] D.P Kothari, I.J Nagrath, *Modern Power System Analysis*, Second Revised Edition, Delhi, India: Tata Mc Graw Hill, 2009.
- [15] C.L Wadhwa, *Electrical Power Systems*, Fifth Edition, Bangalore, India: New Age International Pvt. Ltd., Jan 2009.

APPENDIX A

MESOPOLIS

The virtual city of Mesopolis was designed for the purpose of it being used as a test bed for carrying out studies on the effects of disasters on the interdependent infrastructure components of a city. Mesopolis was developed using GIS (ArcMap) and hydraulic modeling (EPANet) based software [3]. The electrical distribution network of the city was then modeled and its corresponding components added to the GIS layout. Mesopolis, a city of around 100000 residents, covers an area of approximately 2 square miles. To make the design as realistic as possible, a developmental time line of 130 years was taken into consideration. While this time line is manifested by the choice of pipe material, pipe diameter etc. for the civil infrastructure model, it does not have a significant impact on the electrical modeling as most electrical components are either upgraded or replaced after every 30-40 years [7].

- Designing of Mesopolis: Figures 36 and 37 show the sequence of steps involved in developing Mesopolis testbed. Figure 38 shows virtual layout of the city of Mesopolis along with its electrical infrastructure components. It is assumed that Mesopolis has a power generation facility of its own and it is connected with the grid through a sub-transmission line (138 KV rating) running through the city, as shown above. The city has seven substations, where the sub-transmission level voltage of 138 KV is stepped down to the distribution level voltage of 12.47 KV. Two three-phase feeder lines (each of 12.47 KV rating) emanate from the substation, and by repeated branching off into smaller three-phase subsections and finally into single-phase laterals; they deliver the power from the substation across the entire city. Overhead conductors are represented by

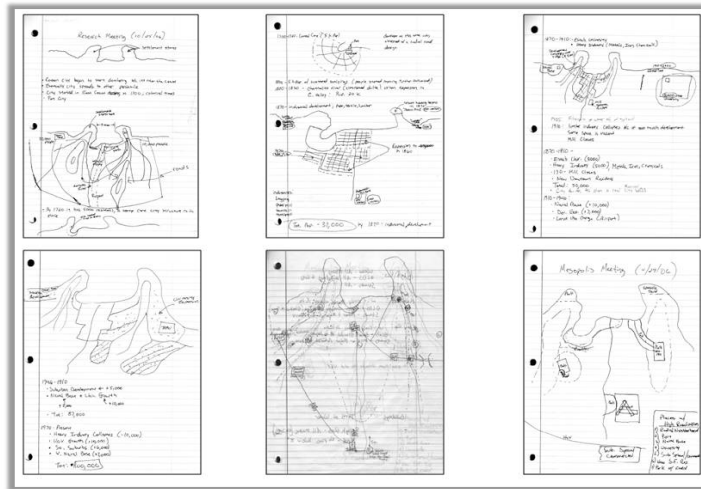


Fig. 36. Paper layouts showing building of Mesopolis

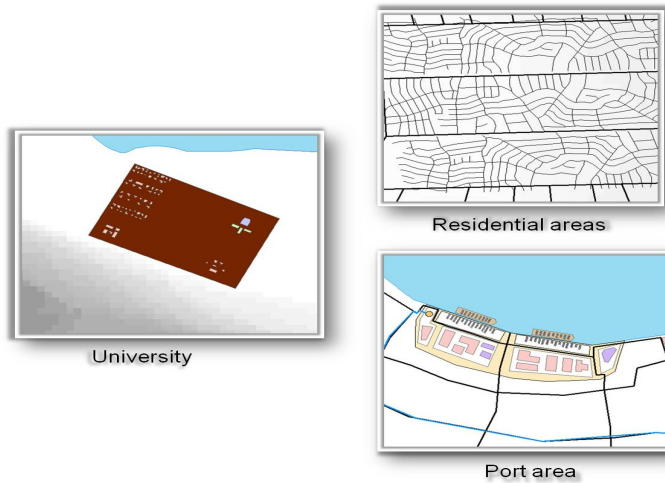


Fig. 37. University, residential areas and port in Mesopolis

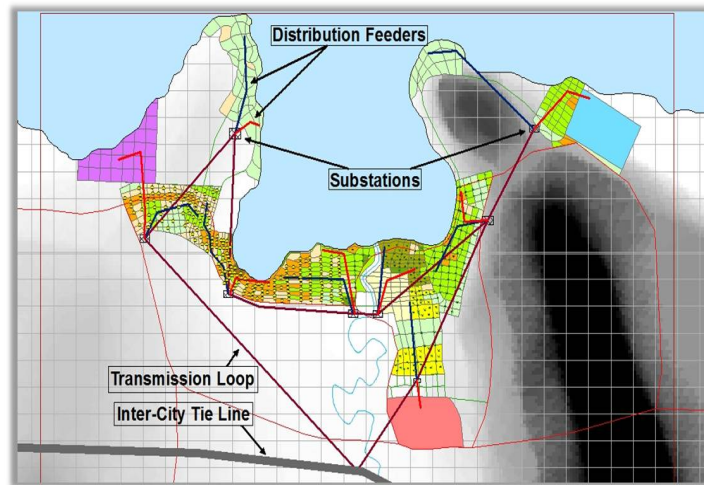


Fig. 38. Overview of Mesopolis

the solid lines while underground cables are shown using dotted lines. The overhead conductors are supported on wooden poles, which are represented by the yellow dots. Distribution transformers rated 100 KVA or above are pad mounted, while others are mounted on the poles unless they are fed by underground cables (in which case they are always pad mounted). All pad mounted distribution transformers are assumed to be enclosed in iron casings. Table XVII shows the voltage profile of customers in Mesopolis. Table XVIII shows the load profile of customers in Mesopolis.

Table XVII. Voltage profile of customers in Mesopolis

Voltage Profiles

| Customer Type | Voltage Ratings |
|---------------------------|---------------------------------------|
| Residential | 120V, 1 – ϕ |
| City Churches and Schools | 208V, 3 – ϕ |
| Industrial | 208V, 3 – ϕ or 3.3KV, 3 – ϕ |
| Central Business District | 208V, 3 – ϕ |

Table XVIII. Load profile of customers in Mesopolis

Load Profiles

| Customer Type | Load Consumed |
|---------------------------|----------------------|
| Residential | 7 KVA |
| City Churches | 250 KVA |
| City Schools | 300 KVA |
| Industrial | 30/75/150/22 KVA |
| Central Business District | 30/45/150/250 KVA |

VITA

Name:

Suraj Chanda

Address:

Department of Electrical and Computer Engineering,

Texas A&M University,

214 Zachry Engineering Center,

Mailstop 3128 TAMU,

College Station, Texas 77843-3128

Email Id:

chandasuraj37@gmail.com

Education:

B.E., Electrical and Electronics Engineering,

Osmania University, Hyderabad, A.P., India, May 2008

M.S., Electrical Engineering, Texas A&M University, Aug. 2011

The typist for this thesis was Suraj Chanda.